Table 1
Reconstitution of human multilineage leukocytes in NOG-hCD34 mice[a,b].

Linage marker[c]	CD45+	CD3+	CD19+	CD4+	CD8+	CD14+	CD34+
PB (12–13-week old)	34.9 ± 11.3	10.2 ± 6.9	17.5 ± 6.3	4.7 ± 2.9	5.2 ± 3.3	n.a.[f]	n.a.
PB (28–31-week old)	33.3 ± 14.5	22.4 ± 6.8	8.7 ± 9.1	14.0 ± 6.2	5.4 ± 2.3	0.2 ± 0.2	n.a.
BM[d]	43.2 ± 20.8	7.8 ± 5.7	27.2 ± 24.6	n.a.	n.a.	2.7 ± 3.2	5.4 ± 3.9
Spleen[d]	75.9 ± 16.4	42.9 ± 22.9	25.6 ± 12.3	26.3 ± 10.6	11.5 ± 8.0	n.a.	n.a.
Lymph nodes[d]	94.8 ± 5.1	82.2 ± 8.7	8.0 ± 4.2	n.a.	n.a.	n.a.	n.a.

Linage marker[e]	CD45+	CD4SP	CD8SP	DP	DN
Thymus[d]	98.5 ± 0.4	12.6 ± 7.7	6.5 ± 4.9	76.3 ± 20.9	10.8 ± 10.6

[a] Each population of human leukocytes in NOG-hCD34 mice ($n = 4$–8) was analyzed by flow cytometry as described in Section 2.
[b] Average percentage of each linage marker positive cell in whole mononuclear cells is shown with standard deviation.
[c] Each linage marker indicates followings: CD45, pan leukocytes; CD3, T lymphocytes; CD19, B lymphocytes; CD14, monocytes; CD34, hematopoietic cells.
[d] Tissues were collected between 28 and 44 weeks old as described in Section 2.
[e] SP, single positive; DP, CD4CD8 double positive; DN, CD4CD8 double negative.
[f] Not analyzed.

(Fig. 1B). These results indicate that HIV-$1_{JR\text{-}CSF}$ was sufficiently replicated in NOG-hCD34 mice.

The PB samples of HIV-$1_{JR\text{-}CSF}$-infected and mock-infected NOG-hCD34 mice were periodically collected and human lymphocytes were sequentially analyzed by flow cytometry. We observed that peripheral $CD4^+$ to $CD8^+$ ratio of HIV-$1_{JR\text{-}CSF}$-infected mice was constantly lower than that of the mock-infected mice (Fig. 1C). Moreover, the percentage of peripheral $CD4^+$ T lymphocytes in both

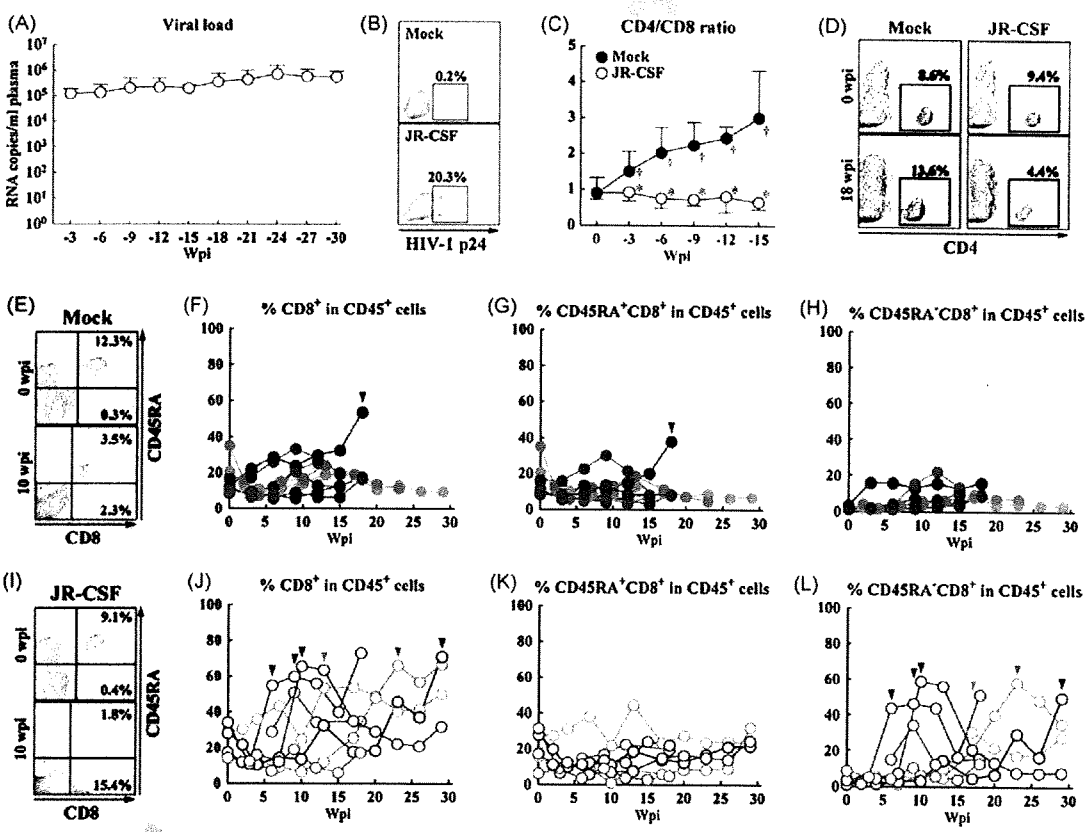

Fig. 1. Immunopathological analyses on CCR5-tropic HIV-1-infected NOG-hCD34 mice. NOG-hCD34 mice were intraperitoneally inoculated with ~~RPMI-1640~~ (for mock infection, filled circles, $n = 8$) or HIV-$1_{JR\text{-}CSF}$ (1×10^5 $TCID_{50}$/mouse, opened circles, $n = 7$) between 12 and 13-week old. (A) The longitudinal analysis on the plasma viral load of HIV-$1_{JR\text{-}CSF}$-infected mice. Plasma was routinely collected and HIV-1 RNA was quantified as described in Section 2. (B) Detection of HIV-1 antigen-expressing cells. Splenic mononuclear cells of mock-infected (top) and HIV-$1_{JR\text{-}CSF}$-infected (bottom) mice were stained with an anti-HIV-1 p24 antibody and analyzed by flow cytometry. A representative results are shown. The percentages in plots indicate the percentage of p24-positive cells in splenic whole mononuclear cells. (C–L) The longitudinal analyses in the PB of mock-infected and HIV-$1_{JR\text{-}CSF}$-infected mice. PB was routinely collected and longitudinally analyzed by flow cytometry. (C) CD4/CD8 ratio in the PB. Broken line in gray indicates CD4/CD8 ratio = 1. (D) Representative profiles of $CD4^+$ T lymphocytes in the PB. The results in the PB of mock-infected (left) and HIV-$1_{JR\text{-}CSF}$-infected (right) mice at 0 wpi (top) and 18 wpi (bottom) are shown. The percentages in plots indicate the percentage of CD4-positive cells in whole mononuclear cells. (E–H) The percentages of whole $CD8^+$ (F and J), naïve $CD45RA^+CD8^+$ (G and K), and memory $CD45RA^-CD8^+$ (H and L) T lymphocytes in the PB of mock-infected (F–H) and HIV-$1_{JR\text{-}CSF}$-infected (J–L) mice are shown. (E and I) Representative profiles of naïve and memory $CD8^+$ T lymphocytes in the PB. The results in the PB of mock-infected (E) and HIV-$1_{JR\text{-}CSF}$-infected (I) mice at 0 wpi (top) and 10 wpi (bottom) are shown. The percentages in each quadrant indicate the percentages of $CD8^+CD45RA^+$ naïve cells (right upper) and $CD8^+CD45RA^-$ memory cells (right lower) in whole mononuclear cells. In panels A and C, the data are assigned into periodic groups (0, 1–3, 4–6, 7–9, 10–12, 13–15, 16–18, 19–21, 22–24, 25–27, and 28–30 wpi). Error bars in panels A and C represent standard deviations. Arrowheads in panels F, G, J, and L indicate distinctive peaks or increases in the percentages of $CD8^+$ T lymphocytes or their subsets. Asterisks represent statistical differences ($P < 0.05$ by Student's t test) versus the values of mock-infected mice at the same time point, and daggers represent statistical differences ($P < 0.05$ by paired t test) versus the value at 0 wpi.

Please cite this article in press as: Sato K, et al. Dynamics of memory and naive $CD8^+$ T lymphocytes in humanized NOD/SCID/IL-2Rγ^{null} mice infected with CCR5-tropic HIV-1. Vaccine (2009), doi:10.1016/j.vaccine.2009.10.154

human CD45$^+$ cells and whole mononuclear cells of mock-infected mice mildly increased, while this increase was not observed in HIV-$1_{JR\text{-}CSF}$-infected mice (Fig. 1D).

3.3. Proliferation of memory CD8$^+$ T lymphocytes in CCR5-tropic HIV-1-infected NOG-hCD34 mice

We also longitudinally analyzed on the percentages of CD8$^+$ T lymphocytes within human CD45$^+$ cells in the PB of mock-infected and HIV-$1_{JR\text{-}CSF}$-infected mice (Fig. 1E–I). CD8$^+$ T lymphocytes were further distinguished into memory and naïve populations on the basis of naïve T-cell marker CD45RA. In the mock-infected mice, the percentages of whole CD8$^+$ (Fig. 1F), CD45RA$^+$CD8$^+$ naïve (Fig. 1G), and memory CD45RA$^-$CD8$^+$ (Fig. 1H) T lymphocytes stayed consistent throughout the investigation with one exception that displayed increase in the percentage of CD8$^+$ T lymphocytes (Fig. 1F). This increase was attributed to an occasional increase in CD45RA$^+$ subset of CD8$^+$ T lymphocytes (Fig. 1G, arrowhead). In contrast, in 6 out of the 7 HIV-$1_{JR\text{-}CSF}$-infected mice, the percentages of whole CD8$^+$ and memory CD45RA$^-$CD8$^+$ T lymphocytes drastically increased after infection displaying distinctive peaks (Fig. 1J and L with arrowheads. A representative result is shown in Fig. 1I), while the percentages of naïve CD45RA$^+$CD8$^+$ T lymphocytes stayed quite stable (Fig. 1K). The peaks in the percentage of CD45RA$^-$CD8$^+$ T lymphocytes directly correlated to those in the percentage of CD8$^+$ T lymphocytes (Fig. 1J and L), indicating that the increase in the CD8$^+$ T lymphocyte population was caused by the increase in the CD45RA$^-$ memory subset.

3.4. Production of antibodies against HIV-1 antigens in CCR5-tropic HIV-1-infected NOG-hCD34 mice

In addition to the proliferative response of memory CD8$^+$ T lymphocytes in HIV-$1_{JR\text{-}CSF}$-infected mice, we found successful differentiation of human CD19$^+$ B lymphocytes in NOG-hCD34 mice (Table 1). To examine whether human antibody response against HIV-1 antigens was induced in the infected mice, we tested the plasma of a mock-infected and 7 HIV-$1_{JR\text{-}CSF}$-infected mice by Western blotting (Fig. 2), which has been clinically utilized for the definitive diagnosis of HIV-1 infection. In the plasma of all NOG-hCD34 mice, human IgG was detected (Fig. 2, lanes 2–4 and not shown), indicating that class-switching of immunoglobulin from IgM to IgG in human B cells occurred. However, we only detected human IgG that reacts with HIV-1 gp41 in the plasma of 2 infected mice (Fig. 2, lanes 3 and 4 with arrowheads). This suggests that generation of humoral immune response against HIV-1 may be limited in the infected mice.

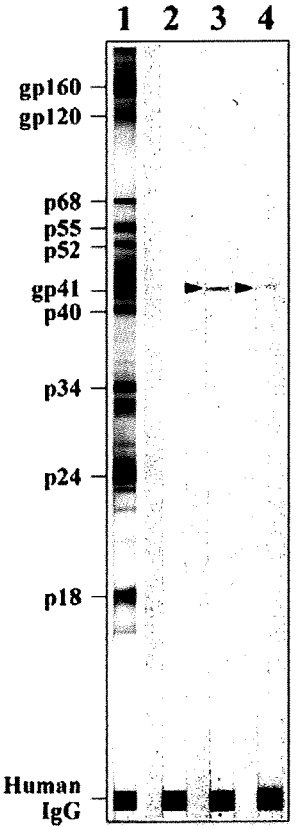

Fig. 2. Production of human IgG and antibodies against HIV-1 antigens in the plasma of CCR5-tropic HIV-1-infected NOG-hCD34 mice. Plasmas were collected from a mock-infected and 7 HIV-$1_{JR\text{-}CSF}$-infected NOG-hCD34 mice upon sacrifice and were examined for the presence of human IgG against HIV-1 antigens as described in Section 2. Representative results from serum of a human HIV-1 positive patient (positive control) (lane 1), and plasmas sampled from a mock-infected (lane 2) and 2 HIV-$1_{JR\text{-}CSF}$-infected (lanes 3 and 4) mice are shown. Arrowheads indicate bands showing the presence of human IgG that reacted with HIV-1 gp41.

4. Discussion

Adult NOG mice have been shown to be able to effectively support *de novo* generation of multilineage human immune cells when transplanted with hHSCs [11–13]. In the present study, we generated NOG-hCD34 mice, which are neonatal NOG mice transplanted with CB-derived hHSCs. These mice produced human T lymphocytes, B lymphocytes, and monocytes, and sustained steady human hematopoiesis for at least 31 weeks (217 days). They were susceptible to infection by HIV-$1_{JR\text{-}CSF}$, and showed high level of persistent viral replication. Furthermore, in addition to the production of HIV-1-specific IgG, human CD8$^+$ T lymphocytes proliferated in HIV-$1_{JR\text{-}CSF}$-infected mice. These suggest that NOG-hCD34 mice have the potential to be of valuable tool for the study of HIV-1 infection *in vivo*.

Classical xenotransplantation of hHSCs in mice used to be unsuccessful in producing *de novo* generated T lymphocytes, because immune cells in recipient mice interfered with hematopoiesis of the transplanted cells [23]. Human T lymphocytes failed to develop even in NOD/SCID mice, a strain of mice considered to have one of the most underdeveloped immune system [24]. The treatment of NOD/SCID mice with anti-NK cell antibody prior to xenotransplantation enhanced the engraftment efficiency, suggesting that NK cells were important mediators of graft failure in NOD/SCID mice [24]. Subsequently, highly immunodeficient strains of mice such as NOG mice and Rag2$^{-/-}\gamma c^{-/-}$ mice were generated and were found to be much better recipients for human grafts [11,15,25]. NOG mice, which are NOD/SCID mice with null mutation at the IL-2Rγ gene, were completely defective in NK cell function [11]. NOG-hCD34 mice supported the differentiation of human leukocytes including T lymphocytes from engrafted hHSCs, and they were shown to support long-term productive infection by HIV-1 [11–15]. In adult NOG mice transplanted with hHSCs, HIV-1 infection resulted in production of HIV-1-specific antibody response [12]. In our study, we transplanted CB-derived hHSCs into neonatal NOG mice by hepatic injection. Neonatal mice are thought to be better recipients for CB-derived hHSCs transplantation with regard to both engraftment and immune reconstitution as compared to their adult counterpart [15,16]. Indeed, like adult NOG mice transplanted with hHSCs, hHSCs in our NOG-hCD34 mice differentiated into mature T lymphocytes, B lymphocytes, monocytes, and DCs (Table 1 and not shown). High level of HIV-1 viremia (Fig. 1A) and HIV-1 antigen-expressing cells (Fig. 1B) were detected in these mice when they were infected with HIV-$1_{JR\text{-}CSF}$. The extent of human immune

Please cite this article in press as: Sato K, et al. Dynamics of memory and naïve CD8$^+$ T lymphocytes in humanized NOD/SCID/IL-2Rγ^{null} mice infected with CCR5-tropic HIV-1. Vaccine (2009), doi:10.1016/j.vaccine.2009.10.154

cell reconstitution, the duration in which the human cells were maintained, and the level of HIV-1 replication were comparable to those observed in the hHSCs-transplanted adult NOG mice [12,13] and hHSCs-transplanted Rag2$^{-/-}\gamma_c^{-/-}$ mice [16]. Class-switching of antibodies and the production of HIV-1-specific IgG were also observed in NOG-hCD34 mice (Fig. 2), as were observed in hHSCs-transplanted adult NOG mice [12]. Moreover, effector/memory CD8$^+$ T lymphocytes proliferated in response to HIV-1 infection (Fig. 1E–L). These data indicate that NOG-hCD34 mice have strong potential as an animal model for HIV-1 infection.

In both humans and mice, ~~T cell~~ precursors are selected in the thymus by thymic epithelial cells and DCs expressing major histocompatibility complexes (MHCs). Previous studies [26] and our findings shown in Table 1 strongly indicate that the human ~~T cells~~ are selected and maturated in the murine thymus as normal T lymphocytes need to recognize MHC molecules presented in the thymus to survive [27]. However, it is still uncertain how human T lymphocytes are selected in the recipient murine thymus by murine MHC molecules. It has been shown that mature T lymphocytes can develop from CB-derived mononuclear cell cultures with supplementation of stem cell factor and interleukin-7 but without thymic feeder cells *in vitro* [28], suggesting that development of human T lymphocytes in humanized mice may be independent of murine MHC molecules. On the other hand, others asserted that murine thymus can support human ~~T cell~~ differentiation via murine MHCs [29,30]. Although it is unclear whether human T lymphocytes *de novo* generated in hHSCs-xenotransplanted humanized mice are selected by human or murine MHCs, it has been reported that T lymphocytes capable of eliciting immune responses can be produced within humanized mice [14,16,23]. For instance, two reports showed that human CD8$^+$ T lymphocytes in the humanized mice infected with Epstein–Barr virus (EBV) massively proliferated, and that the CD8$^+$ T lymphocytes were reactivated *in vitro* by EBV antigens presented on human MHCs to some extent [16,31]. We have also observed the activation and the proliferation of human CD8$^+$ T lymphocytes in EBV-infected NOG-hCD34 mice (our unpublished observation). Although whether these CD8$^+$ ~~T cells~~ can elicit human MHC-restricted EBV-specific cytotoxic activity is still under investigation, these findings suggest that human CD8$^+$ T lymphocytes differentiated *de novo* in humanized mice may be selected and primed, at least partly, through human MHCs.

CD8$^+$ T lymphocytes can recognize viral peptides bound to MHC class I molecules and induce cytotoxicity against cells bearing the peptide/MHC class I complex, thus eliminating infected cells [32]. It is thought that CD8$^+$ T lymphocyte-mediated immune surveillance plays an important role in fighting against HIV-1 infection [33]. However, naïve CD8$^+$ T lymphocytes are not able to induce cytotoxicity and only become capable of cell killing after priming by antigen presenting cells (APCs) [34]. The priming of CD8$^+$ T lymphocytes requires complex interactions that include the ligation with both antigen peptide-loaded MHC class I and co-stimulatory molecules on APCs [34]. Successful priming of CD8$^+$ T lymphocytes lead to activation and proliferation of CD8$^+$ T lymphocytes, as well as down-regulation of surface CD45RA molecules [34,35]. The proliferation of CD8$^+$ T lymphocytes lacking CD45RA expression (effector/memory CD8$^+$ T lymphocytes) in HIV-1-infected humanized mice suggests that *de novo* generated leukocytes may be able to initiate and maintain HIV-1-specific CD8$^+$ T lymphocyte responses. Although the proliferation of effector/memory CD8$^+$ T lymphocytes was not associated with the reduction in plasma viral load, it is encouraging to know that such a CD8$^+$ T lymphocyte-mediated response against HIV-1 can be produced in hHSCs-transplanted NOG mice. As far as we know, the proliferation of effector/memory CD8$^+$ T lymphocytes in HIV-1 infection has not been reported in hHSCs-transplanted adult NOG mice [12,13], which may offer a broader application for NOG mice that receive neonatal transplantation. The generation of HIV-1-specific adaptive immune responses makes the present NOG-hCD34 mice system a possible candidate for HIV-1 vaccine evaluation.

Being able to allow HIV-1 replication makes hHSCs-transplanted NOG mice a good candidate for the evaluation of anti-HIV-1 drugs. However, it is not known whether hHSCs-transplanted NOG mice provided researchers with ideal system to study the interaction between human leukocytes and HIV-1. Both viral distraction of CD4$^+$ T lymphocytes and dysregulation of lymphocyte homeostasis are thought to contribute to immune deficiency caused by HIV-1 [36–38]. Therefore, it is important to study the effect of HIV-1 on different subsets of lymphocytes using NOG-hCD34 mice. We found that significant amount of both memory and naïve T lymphocytes were produced in NOG-hCD34 mice (data not shown). In addition, we also found that CCR5-tropic HIV-1 infection caused significant depletion of the memory but not the naïve subset of CD4$^+$ T lymphocytes in the periphery, which resulted in the reduction in overall CD4$^+$ T lymphocytes (Fig. 1C and D) (Nie et al., unpublished data). Furthermore, we found that CD4$^+$ T lymphocytes bearing CCR5 were severely reduced in the spleen of HIV-1-infected mice (Nie et al., unpublished data). These suggest that NOG-hCD34 mice can be used to study the dysregulation of CD4$^+$ T lymphocyte homeostasis after ~~HIV infection~~.

The emergence of severely immunodeficient mice, such as NOG mice and Rag2$^{-/-}\gamma_c^{-/-}$ mice, which can produce human T lymphocytes upon hHSCs transplantation, has made more sophisticated *in vivo* analyses on HIV-1 infection possible. However, the potential of these models to simulate HIV-1 infection and anti-HIV-1 immune response in human is to be explored in detail. Future investigations should include more thorough analyses on *de novo* reconstituted human immune system and how it is altered by HIV-1 infection, so that we can fully utilize this valuable tool.

Acknowledgements

We would like to thank Hiroko Kitayama (Institute for Virus Research, Kyoto University), Hisanori Fujino, Hidefumi Hiramatsu, Toshio Heike, and Tatsutoshi Nakahata (Graduate School of Medicine, Kyoto University) for helping our study. We also would like to express our appreciation for Ms. Kotubu Misawa's dedicated support. This work was supported by Grant-in-Aid for Scientific Research on Priority Areas from the Ministry of Education, Culture, Sports, Sciences, and Technology of Japan, and a Health and Labor Science Research Grant (Research on Publicly Essential Drugs and Medical Devices) from the Ministry of Health, Labor and Welfare of Japan and Japan Human Science Foundation. K.S. was supported by Research Fellowships of the Japan Society for the Promotion of Science for Young Scientists. Y.K. was supported by a grant from the Naito Foundation.

References

[1] Fauci AS. The human immunodeficiency virus: infectivity and mechanisms of pathogenesis. Science 1988;239(4840):617–22.
[2] Jamieson BD, Zack JA. Murine models for HIV disease. AIDS 1999;13(Suppl. A):S5–11.
[3] van Maanen M, Sutton RE. Rodent models for HIV-1 infection and disease. Curr HIV Res 2003;1(1):121–30.
[4] McCune J, Kaneshima H, Krowka J, Namikawa R, Outzen H, Peault B, et al. The SCID-hu mouse: a small animal model for HIV infection and pathogenesis. Annu Rev Immunol 1991;9:399–429.
[5] Namikawa R, Kaneshima H, Lieberman M, Weissman IL, McCune JM. Infection of the SCID-hu mouse by HIV-1. Science 1988;242(4886):1684–6.
[6] Kaneshima H, Shih CC, Namikawa R, Rabin L, Outzen H, Machado SG, et al. Human immunodeficiency virus infection of human lymph nodes in the SCID-hu mouse. Proc Natl Acad Sci USA 1991;88(10):4523–7.
[7] Mosier DE, Gulizia RJ, Baird SM, Wilson DB, Spector DH, Spector SA. Human immunodeficiency virus infection of human-PBL-SCID mice. Science 1991;251(4995):791–4.

Please cite this article in press as: Sato K, et al. Dynamics of memory and naïve CD8$^+$ T lymphocytes in humanized NOD/SCID/IL-2Rγ^{null} mice infected with CCR5-tropic HIV-1. Vaccine (2009), doi:10.1016/j.vaccine.2009.10.154

[8] Jenkins M, Hanley MB, Moreno MB, Wieder E, McCune JM. Human immunodeficiency virus-1 infection interrupts thymopoiesis and multilineage hematopoiesis *in vivo*. Blood 1998;91(8):2672–8.
[9] Berkowitz RD, Alexander S, Bare C, Linquist-Stepps V, Bogan M, Moreno ME, et al. CCR5- and CXCR4-utilizing strains of human immunodeficiency virus type 1 exhibit differential tropism and pathogenesis *in vivo*. J Virol 1998;72(12):10108–17.
[10] Fais S, Lapenta C, Santini SM, Spada M, Parlato S, Logozzi M, et al. Human immunodeficiency virus type 1 strains R5 and X4 induce different pathogenic effects in hu-PBL-SCID mice, depending on the state of activation/differentiation of human target cells at the time of primary infection. J Virol 1999;73(8):6453–9.
[11] Ito M, Hiramatsu H, Kobayashi K, Suzue K, Kawahata M, Hioki K, et al. NOD/SCID/γ_c^{null} mouse: an excellent recipient mouse model for engraftment of human cells. Blood 2002;100(9):3175–82.
[12] Watanabe S, Terashima K, Ohta S, Horibata S, Yajima M, Shiozawa Y, et al. hematopoietic stem cell-engrafted NOD/SCID/IL2Rγ^{null} mice develop human lymphoid system and induce long-lasting HIV-1 infection with specific humoral immune responses. Blood 2007;109(1):212–8.
[13] Watanabe S, Ohta S, Yajima M, Terashima K, Ito M, Mugishima H, et al. Humanized NOD/SCID/IL2Rγ^{null} mice transplanted with hematopoietic stem cells under nonmyeloablative conditions show prolonged life spans and allow detailed analysis of human immunodeficiency virus type 1 pathogenesis. J Virol 2007;81(23):13259–64.
[14] Hiramatsu H, Nishikomori R, Heike T, Ito M, Kobayashi K, Katamura K, et al. Complete reconstitution of human lymphocytes from cord blood CD34$^+$ cells using the NOD/SCID/γ_c^{null} mice model. Blood 2003;102(3):873–80.
[15] Ishikawa F, Yasukawa M, Lyons B, Yoshida S, Miyamoto T, Yoshimoto G, et al. Development of functional human blood and immune systems in NOD/SCID/IL2 receptor γ chain^{null} mice. Blood 2005;106(5):1565–73.
[16] Traggiai E, Chicha L, Mazzucchelli L, Bronz L, Piffaretti JC, Lanzavecchia A, et al. Development of a human adaptive immune system in cord blood cell-transplanted mice. Science 2004;304(5667):104–7.
[17] Koyanagi Y, Miles S, Mitsuyasu RT, Merrill JE, Vinters HV, Chen IS. Dual infection of the central nervous system by AIDS viruses with distinct cellular tropisms. Science 1987;236(4803):819–22.
[18] Koyanagi Y, Tanaka Y, Kira J, Ito M, Hioki K, Misawa N, et al. Primary human immunodeficiency virus type 1 viremia and central nervous system invasion in a novel hu-PBL-immunodeficient mouse strain. J Virol 1997;71(3):2417–24.
[19] Sato K, Aoki J, Misawa N, Daikoku E, Sano K, Tanaka Y, et al. Modulation of human immunodeficiency virus type 1 infectivity through incorporation of tetraspanin proteins. J Virol 2008;82(2):1021–33.
[20] Okuma K, Tanaka R, Ogura T, Ito M, Kumakura S, Yanaka M, et al. Interleukin-4-transgenic hu-PBL-SCID mice: a model for the screening of antiviral drugs and immunotherapeutic agents against X4 HIV-1 viruses. J Infect Dis 2008;197(1):134–41.
[21] Dejucq N, Simmons G, Clapham PR. Expanded tropism of primary human immunodeficiency virus type 1 R5 strains to CD4$^+$ T-cell lines determined by the capacity to exploit low concentrations of CCR5. J Virol 1999;73(9):7842–7.
[22] Hockett RD, Kilby JM, Derdeyn CA, Saag MS, Sillers M, Squires K, et al. Constant mean viral copy number per infected cell in tissues regardless of high, low, or undetectable plasma HIV RNA. J Exp Med 1999;189(10):1545–54.
[23] Legrand N, Weijer K, Spits H. Experimental models to study development and function of the human immune system *in vivo*. J Immunol 2006;176(4):2053–8.
[24] Kerre TC, De Smet G, De Smedt M, Zippelius A, Pittet MJ, Langerak AW, et al. Adapted NOD/SCID model supports development of phenotypically and functionally mature T cells from human umbilical cord blood CD34$^+$ cells. Blood 2002;99(5):1620–6.
[25] Gimeno R, Weijer K, Voordouw A, Uittenbogaart CH, Legrand N, Alves NL, et al. Monitoring the effect of gene silencing by RNA interference in human CD34$^+$ cells injected into newborn RAG2$^{-/-}\gamma_c^{-/-}$ mice: functional inactivation of p53 in developing T cells. Blood 2004;104(13):3886–93.
[26] Macchiarini F, Manz MG, Palucka AK, Shultz LD. Humanized mice: are we there yet? J Exp Med 2005;202(10):1307–11.
[27] Liu YJ. A unified theory of central tolerance in the thymus. Trends Immunol 2006;27(5):215–21.
[28] Sanchez M, Alfani E, Visconti G, Passarelli AM, Migliaccio AR, Migliaccio G. Thymus-independent T-cell differentiation *in vitro*. Br J Haematol 1998;103(4):1198–205.
[29] Robin C, Bennaceur-Griscelli A, Louache F, Vainchenker W, Coulombel L. Identification of human T-lymphoid progenitor cells in CD34$^+$ CD38^{low} and CD34$^+$ CD38$^+$ subsets of human cord blood and bone marrow cells using NOD-SCID fetal thymus organ cultures. Br J Haematol 1999;104(4):809–19.
[30] Weekx SF, Snoeck HW, Offner F, De Smedt M, Van Bockstaele DR, Nijs G, et al. Generation of T cells from adult human hematopoietic stem cells and progenitors in a fetal thymic organ culture system: stimulation by tumor necrosis factor-α. Blood 2000;95(9):2806–12.
[31] Yajima M, Imadome KI, Nakagawa A, Watanabe S, Terashima K, Nakamura H, et al. A new humanized mouse model of Epstein-Barr virus infection that reproduces persistent infection, lymphoproliferative disorder, and cell-mediated and humoral immune responses. J Infect Dis 2008;198(5):673–82.
[32] Hislop AD, Taylor GS, Sauce D, Rickinson AB. Cellular responses to viral infection in humans: lessons from Epstein-Barr virus. Annu Rev Immunol 2007;25:587–617.
[33] Vasan S, Schlesinger SJ, Arrode G. T cell immune responses to HIV-1. Front Biosci 2007;12:2330–43.
[34] Steinman RM. The dendritic cell system and its role in immunogenicity. Annu Rev Immunol 1991;9:271–96.
[35] Clement LT. Isoforms of the CD45 common leukocyte antigen family: markers for human T-cell differentiation. J Clin Immunol 1992;12(1):1–10.
[36] Centlivre M, Sala M, Wain-Hobson S, Berkhout B. In HIV-1 pathogenesis the die is cast during primary infection. AIDS 2007;21(1):1–11.
[37] Brenchley JM, Schacker TW, Ruff LE, Price DA, Taylor JH, Beilman GJ, et al. CD4$^+$ T cell depletion during all stages of HIV disease occurs predominantly in the gastrointestinal tract. J Exp Med 2004;200(6):749–59.
[38] Okoye A, Meier-Schellersheim M, Brenchley JM, Hagen SI, Walker JM, Rohankhedkar M, et al. Progressive CD4$^+$ central memory T cell decline results in CD4$^+$ effector memory insufficiency and overt disease in chronic SIV infection. J Exp Med 2007;204(9):2171–85.

Please cite this article in press as: Sato K, et al. Dynamics of memory and naïve CD8$^+$ T lymphocytes in humanized NOD/SCID/IL-2Rγ^{null} mice infected with CCR5-tropic HIV-1. Vaccine (2009), doi:10.1016/j.vaccine.2009.10.154

Journal of General Virology (2010), 91, 773–781 DOI 10.1099/vir.0.017368-0

Small intestine CD4$^+$ cell reduction and enteropathy in simian/human immunodeficiency virus KS661-infected rhesus macaques in the presence of low viral load

Katsuhisa Inaba,[1] Yoshinori Fukazawa,[1] Kenta Matsuda,[1] Ai Himeno,[1] Megumi Matsuyama,[1] Kentaro Ibuki,[1] Yoshiharu Miura,[2] Yoshio Koyanagi,[2] Atsushi Nakajima,[3] Richard S. Blumberg,[4] Hidemi Takahashi,[5] Masanori Hayami,[1] Tatsuhiko Igarashi[1] and Tomoyuki Miura[1]

Correspondence
Tomoyuki Miura
tmiura@virus.kyoto-u.ac.jp

[1]Laboratory of Primate Model, Experimental Research Center for Infectious Diseases, Institute for Virus Research, Kyoto University, 53 Shogoinkawaramachi, Sakyo-ku, Kyoto 606-8507, Japan

[2]Laboratory of Viral Pathogenesis, Institute for Virus Research, Kyoto University, 53 Shogoinkawaramachi, Sakyo-ku, Kyoto 606-8507, Japan

[3]Division of Gastroenterology, Yokohama City University Graduate School of Medicine, Yokohama, Japan

[4]Division of Gastroenterology, Brigham and Women's Hospital, Harvard Medical School, Boston, MA, USA

[5]Department of Microbiology and Immunology, Nippon Medical School, Tokyo, Japan

Human immunodeficiency virus type 1, simian immunodeficiency virus and simian/human immunodeficiency virus (SHIV) infection generally lead to death of the host accompanied by high viraemia and profound CD4$^+$ T-cell depletion. SHIV clone KS661-infected rhesus macaques with a high viral load set point (HVL) ultimately experience diarrhoea and wasting at 6–12 months after infection. In contrast, infected macaques with a low viral load set point (LVL) usually live asymptomatically throughout the observation period, and are therefore referred to as asymptomatic LVL (Asym LVL) macaques. Interestingly, some LVL macaques exhibit diarrhoea and wasting similar to the symptoms of HVL macaques and are termed symptomatic LVL (Sym LVL) macaques. This study tested the hypothesis that Sym LVL macaques have the same degree of intestinal abnormalities as HVL macaques. The proviral DNA loads in lymphoid tissue and the intestines of Sym LVL and Asym LVL macaques were comparable and all infected monkeys showed villous atrophy. Notably, the CD4$^+$ cell frequencies of lymphoid tissues and intestines in Sym LVL macaques were remarkably lower than those in Asym LVL and uninfected macaques. Furthermore, Sym LVL and HVL macaques exhibited an increased number of activated macrophages. In conclusion, intestinal disorders including CD4$^+$ cell reduction and abnormal immune activation can be observed in SHIV-KS661-infected macaques independent of virus replication levels.

Received 5 October 2009
Accepted 3 November 2009

INTRODUCTION

The intestinal tract, which is the largest mucosal and lymphoid organ and which contains the majority of the total lymphocytes in the body, is an important port of entry for human immunodeficiency virus type 1 (HIV-1) infection in vertical and homosexual transmission (Smith *et al.*, 2003). Additionally, the intestinal tract is a central site in the interaction between HIV-1 and its host, and suffers profound pathological changes as a result of HIV-1 infection. HIV-1 infection of the intestinal tract is characterized by virus replication (Fackler *et al.*, 1998), CD4$^+$ T-cell depletion (Brenchley *et al.*, 2004), opportunistic infection and HIV enteropathy, which is an idiopathic intestinal disorder observed in infected patients with diarrhoea (Kotler, 2005). In particular, CD4$^+$ T-cell depletion, which is the immunological hallmark in the development of AIDS, preferentially takes place in the intestinal tract rather than in the peripheral blood throughout the infection (Brenchley *et al.*, 2004). This

017368 © 2010 SGM *Printed in Great Britain*

observation is based on the following findings: (i) most naturally transmitted HIV-1 strains are chemokine receptor 5 (CCR5)-tropic; and (ii) the intestinal tract, especially the lamina propria, contains a large number of activated memory $CCR5^+$ $CD4^+$ T cells, which indicates a high susceptibility for HIV-1 infection, whereas the peripheral blood has a relatively small population of these cells (Anton *et al.*, 2000; Lapenta *et al.*, 1999). $CD4^+$ T-cell depletion from the intestinal tract by HIV-1 infection is thought to lead to progressive dysfunction of mucosal immunity, which triggers immunodeficiency (Paiardini *et al.*, 2008). In addition to $CD4^+$ T-cell depletion in the intestinal tract, HIV-1 infection causes histopathological changes in the intestine, including villous atrophy, crypt hyperplasia and acute/chronic inflammation (Batman *et al.*, 1989).

Chronic disease of the intestinal tract generally manifests as inflammation (Kahn, 1997). Diarrhoea is a major intestinal symptom caused by various stimuli to the intestinal tract such as pathogens, toxins and dysfunction of the immune system (Gibbons & Fuchs, 2007). Because HIV-1 infection weakens the host immune system, AIDS is one of the primary causes of chronic diarrhoea (Sestak, 2005). In developing countries, diarrhoea was a major symptom in advanced HIV-1 infection prior to the establishment of highly active antiretroviral therapy (HAART) (Wilcox & Saag, 2008). Dehydration and malabsorption as a result of chronic diarrhoea can lead to progressive weight loss and can contribute to morbidity and mortality in HIV-1-infected patients (Sharpstone & Gazzard, 1996). Therefore, chronic diarrhoea is one of the most important clinical signs in AIDS patients.

AIDS models using non-human primates have provided many important observations on AIDS pathogenesis. The first finding of early $CD4^+$ T-cell depletion from the intestinal tract was reported in a study using simian immunodeficiency virus (SIV)-infected macaques (Veazey *et al.*, 1998). Intestinal $CD4^+$ T cells of rhesus macaques predominantly exhibit a $CCR5^+$ activated memory phenotype, and $CD4^+$ T cells of this phenotype are selectively eliminated in SIV-infected macaques, indicating that the majority of intestinal $CD4^+$ T cells are primary targets of SIV infection (Veazey *et al.*, 2000a, b). Accordingly, detailed analysis of the intestinal tract using animal models is essential for an understanding of AIDS pathogenesis.

Simian/human immunodeficiency virus (SHIV)-KS661 is a molecular clone and a pathogenic virus in rhesus macaques. SHIV-KS661 systemically depletes $CD4^+$ T cells of rhesus macaques within 4 weeks of infection (Miyake *et al.*, 2006). Based on our observations over a number of years, intravenous infection of rhesus macaques with SHIV-KS661 consistently results in high viraemia and $CD4^+$ T-cell depletion, followed by malignant morbidity as a result of severe chronic diarrhoea and wasting after 6–18 months. Generally, the time to clinical morbidity in rhesus macaques infected with pathogenic SHIVs, such as SHIV-89.6P and SHIV-KS661, is considerably shorter than in HIV-1-infected humans, who take an average of 10 years to progress to AIDS. In addition, all subsets of $CD4^+$ T cells including memory and naïve T cells are thoroughly depleted in pathogenic SHIV-infected macaques. However, in the SHIV-KS661 macaque model, diarrhoea and wasting, which are major symptoms in advanced HIV-1 infection, can clearly be recognized and defined in association with disease progression.

Recently, we observed that, in many rhesus macaques infected intrarectally with SHIV-KS661, plasma viral RNA loads decreased gradually to undetectable levels in the chronic phase, which is quite different from the case with intravenous infection. It is well known that pathogenic SIV and SHIV infections in monkeys, like HIV-1 infections in humans, generally lead to high viraemia, profound $CD4^+$ T-cell depletion and death. Interestingly, in this study, two out of six intrarectally inoculated macaques with a low plasma viral load experienced malignant morbidity manifest as severe diarrhoea and wasting, similar to what we observed in infected macaques with high viraemia. The purpose of this study was to elucidate why macaques with a low plasma viral load experienced diarrhoea and wasting. As an explanation for this morbidity, we hypothesized that, even if the viral load set-point is suppressed, SHIV-KS661-infected macaques would have the same degree of intestinal abnormalities as infected macaques with high viraemia. To test this hypothesis, we analysed $CD4^+$ cell frequencies in lymphoid and intestinal tissues and damage to the intestinal mucosa in infected macaques with high and low viral load set points (HVL and LVL, respectively). Here, we have provided evidence for the development of intestinal disorders in SHIV-KS661-infected macaques irrespective of the plasma viral RNA load.

RESULTS

Diarrhoea and wasting in two macaques despite low viral load

All macaques inoculated intravenously with SHIV-KS661 and one out of seven macaques inoculated intrarectally with SHIV-KS661 exhibited high set points of plasma viral RNA loads, persisting at over 10^6 copies ml^{-1} until they needed to be euthanized as a result of diarrhoea and wasting (Fig. 1a). In contrast, in the remaining six macaques inoculated intrarectally with SHIV-KS661, the set points of plasma viral RNA load gradually decreased to undetectable levels (Fig. 1a). We called these macaques showing high and low set points of viral RNA load HVL and LVL macaques, respectively. During an observation period of approximately 1.4 years, two LVL macaques (MM397 and MM399) experienced severe diarrhoea and wasting and required euthanasia at approximately 22 weeks post-infection (p.i.), similar to HVL macaques, whereas the remaining four LVL macaques were asymptomatic (Fig. 1a). We termed the healthy LVL macaques asymptomatic LVL macaques (Asym LVL) and the LVL

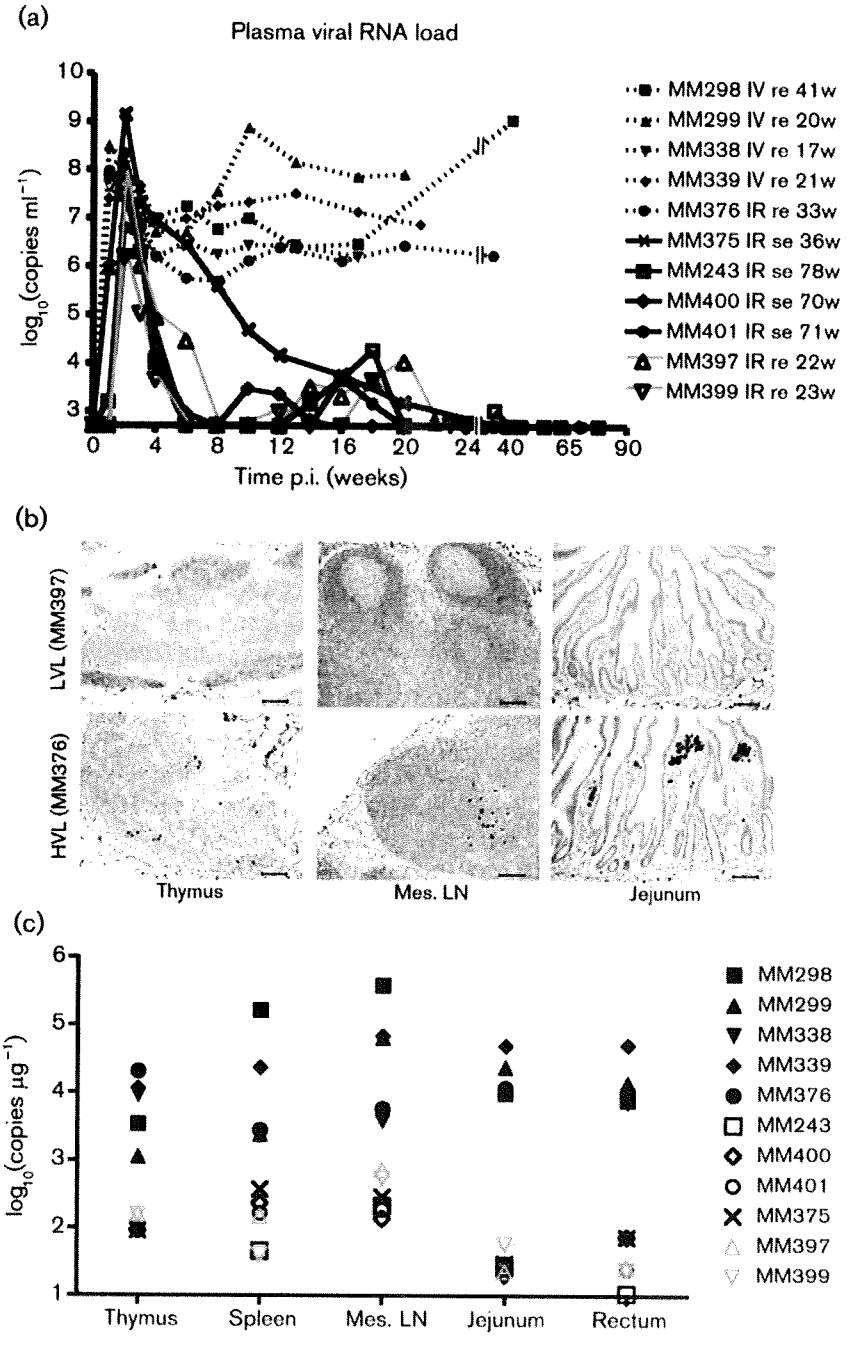

Fig. 1. Distribution of virus in various tissues of SHIV-KS661-infected rhesus macaques. (a) Time course of plasma viral RNA loads as measured by quantitative RT-PCR. The detection limit of plasma viral RNA loads was 500 copies ml^{-1}. The animal ID numbers, infection route and when and how they were euthanized are indicated on the figure. IV, Intravenous inoculation; IR, intrarectal inoculation; re, required euthanasia; se, scheduled euthanasia; w, number of weeks after infection when euthanasia was performed. (b) Immunohistochemical detection of Nef antigen in thymus, mesenteric lymph nodes (Mes. LN) and jejunum. Brown staining indicates Nef^+ cells. The upper panels show representative tissue sections from a Sym LVL macaque (MM397) and the lower panels show representative tissue sections from an HVL macaque (MM376). Bars, 100 µm. (c) Proviral DNA loads in different tissues of SHIV-KS661-infected macaques, as measured by quantitative PCR. The detection limit of proviral DNA loads was 10 copies μg^{-1}. Filled black symbols indicate HVL macaques, open black symbols indicate Asym LVL macaques and open grey symbols indicate Sym LVL macaques.

macaques with diarrhoea and wasting symptomatic LVL macaques (Sym LVL).

Antibody response against SHIV in infected macaques

The LVL macaques showed antibody responses to SHIV-KS661 at 3–4 weeks p.i. and then developed strong antibody responses that persisted up to 18 weeks p.i. (Table 1). In contrast, two of the HVL macaques (MM298 and MM299) showed no antibody response, whilst the remaining two (MM338 and MM339) showed very low antibody responses. Among the HVL macaques, only MM376 showed a strong antibody response: the titre reached 1:2048 at 6 weeks p.i., but then decreased to a much lower value. These results showed that LVL macaques succeeded in maintaining a strong antibody response, whilst HVL macaques failed to do so.

Viral levels in tissues from Sym LVL and Asym LVL macaques are not significantly different

To investigate whether the infected macaques had different viral levels in their lymphoid and intestinal tissues, we used

Table 1. Anti-HIV antibody titres in infected monkeys

– indicates a titre of <32.

Time (weeks)	Intrarectal inoculation						Intravenous inoculation			
	LVL						HVL			
	MM243	MM397	MM399	MM400	MM401	MM375	MM376	MM298	MM299	MM338	MM339
0	–	–	–	–	–	–	–	–	–	–	–
1	–	–	–	–	–	–	–	–	–	–	–
2	–	–	–	–	–	–	–	–	–	64	64
3	32	–	32	–	–	128	–	–	–	32	32
4	32	16384	32	64	32	512	512	–	–	–	–
6	8192	16384	256	64	4096	1024	2048	–	–	–	–
8	4096	16384	1024	128	1024	16384	512	–	–	–	–
10	16384	16384	2048	512	512	16384	512	–	–	–	–
12	16384	16384	256	512	4096	16384	512				
13								–	–	–	–
14	16384	16384	1024	512	2048						
16	4096	8192	1024	1024	1024	16384	64				
17								–	–	–	–
18	8192	16384	2048	8192	4096						

the Nef antigen as a marker of virus infection using immunohistochemistry and quantitative analysis of proviral DNA in lymphoid and intestinal tissues. Nef^+ cells were detected in large numbers in the tissues of HVL macaques, but were undetectable in both Sym LVL (Fig. 1b) and Asym LVL (data not shown) macaques.

In the HVL macaques, high proviral DNA loads (>1000 copies μg^{-1}) were found in all of the tissues examined (Fig. 1c). In contrast, the proviral DNA loads in the tissues of the LVL macaques were only several tens to several hundreds of copies μg^{-1} (Fig. 1c). Furthermore, Sym LVL and Asym LVL macaques exhibited comparably low proviral DNA loads in these tissues (Fig. 1c). The low viral levels in lymphoid and intestinal tissues in the LVL macaques were consistent with their set points of plasma viral RNA loads. The viral levels in lymphoid and intestinal tissues were not significantly different between Sym LVL and Asym LVL macaques.

Diarrhoea and wasting in LVL macaques correlate with $CD4^+$ cell frequency in lymphoid and intestinal tissues, but not in peripheral blood

Because $CD4^+$ T-cell depletion is the hallmark of AIDS, we first examined $CD4^+$ T-cell counts in peripheral blood. Whilst peripheral $CD4^+$ T cells were completely and irreversibly depleted in HVL macaques throughout the infection, they displayed various kinetics in LVL macaques (Fig. 2a). MM397 (Sym LVL) and MM401 (Asym LVL) had very low $CD4^+$ T-cell counts (<150 cells ml^{-1}) at all times at which they were examined after infection, whereas MM399 (Sym LVL) and MM400 (Asym LVL) maintained moderate $CD4^+$ T-cell counts (>300 cells ml^{-1}) throughout the experiment (Fig. 2a).

Naïve $CD4^+$ T cells of MM397 (Sym LVL), MM243 (Asm LVL) and MM401 (Asym LVL) were depleted as early as 4 weeks p.i., whereas those of MM399 (Sym LVL) and MM400 (Asym LVL) remained at moderate levels (Fig. 2b). The HVL macaques were not examined because their peripheral $CD4^+$ T cells were depleted.

In addition to evaluating $CD4^+$ T cells in the blood, we evaluated $CD4^+$ cells in lymphoid and intestinal tissues using CD4 staining. The HVL macaques showed severe depletion of $CD4^+$ cells in all lymphoid tissues and intestine compared with the uninfected macaques (Fig. 2c, d). Interestingly, the $CD4^+$ cell frequencies in the tissues were clearly lower in Sym LVL macaques than in uninfected macaques (Fig. 2c, d). However, the $CD4^+$ cell frequencies in the tissues of Asym LVL macaques were comparable to those in uninfected macaques. These findings indicated that the emergence of diarrhoea and wasting in LVL macaques correlated with the low $CD4^+$ cell frequency in lymphoid tissues and the intestines, but not with the counts of peripheral $CD4^+$ T-cell subsets.

Infected animals exhibit significantly shorter villi

Symptomatic animals (Sym LVL and HVL macaques) exhibited diarrhoea. To examine whether the jejunum of symptomatic animals exhibited the histopathological changes that suggest AIDS-related enteropathy, we measured villous length on haematoxylin and eosin (H&E)-stained samples of jejunum in uninfected and infected macaques. Surprisingly, villous length was significantly

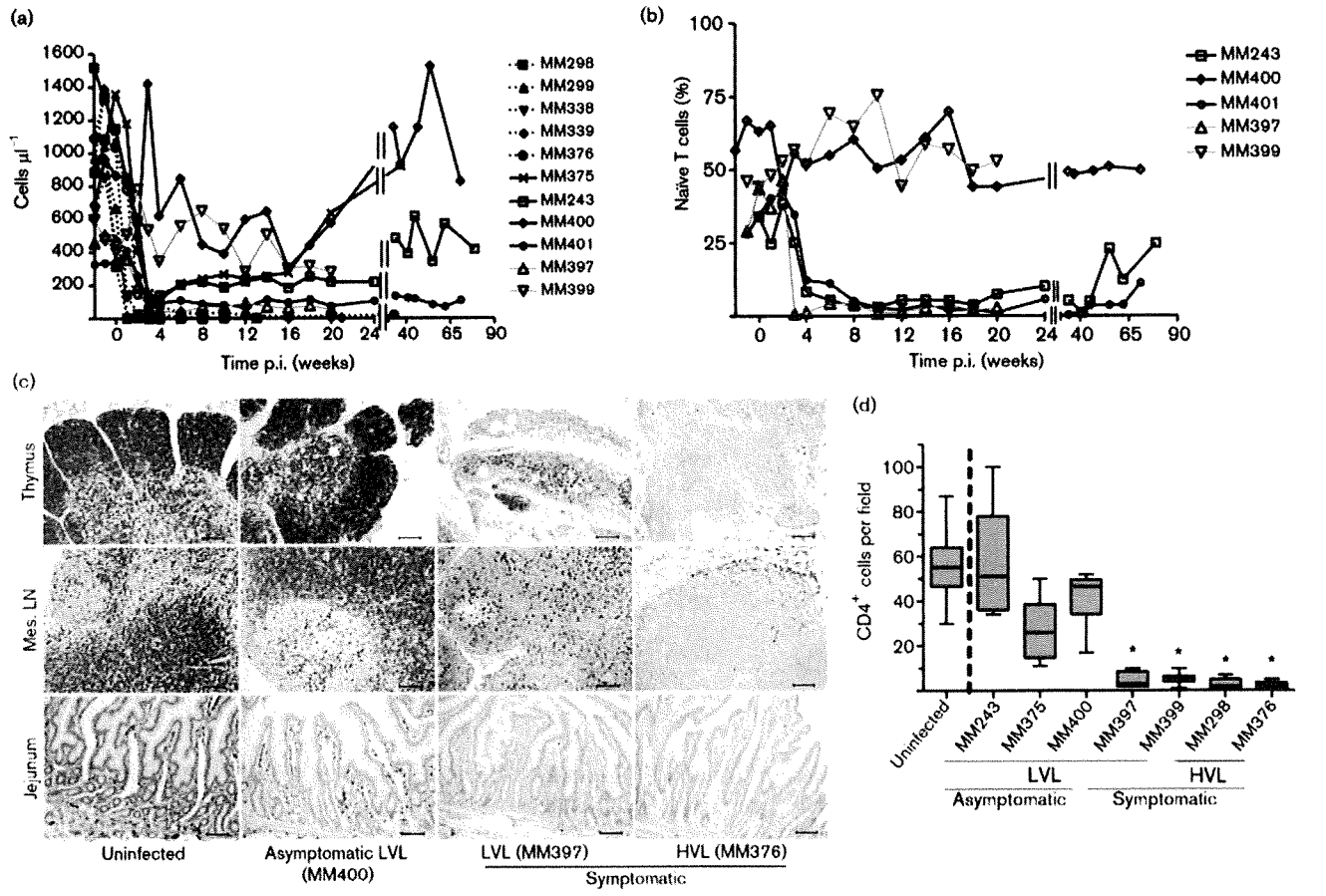

Fig. 2. Counts of circulating $CD4^+$ T-cell subsets and $CD4^+$ cell frequency in lymphoid and intestinal tissues at the time of euthanasia in SHIV-KS661-infected rhesus macaques. Counts of circulating $CD4^+$ T-cell subsets were analysed by flow cytometry and whole-blood counts. (a) Circulating $CD4^+$ T-cell counts. The ID numbers of the macaques are indicated on the figure. (b) Proportion of $CD95^+$ naïve cells in circulating $CD4^+$ T cells of LVL macaques. Solid black lines indicate Asym LVL macaques and solid grey lines indicate Sym LVL macaques. (c) $CD4^+$ cell frequencies in thymus, mesenteric lymph nodes (Mes. LN) and jejunum of representative uninfected, Asym LVL, Sym LVL and HVL macaques. Bars, 100 μm. (d) Quantification of jejunum $CD4^+$ cells in uninfected and infected macaques. The numbers of $CD4^+$ cells were enumerated in at least ten fields of the tissues at a magnification of 200×. Statistical analysis was performed using Student's *t*-test for the data from five uninfected and each infected macaque (*, $P<0.0001$). Data for MM299, MM338, MM339 and MM401 were not available.

shorter in all of the infected animals than in uninfected animals ($P<0.0001$) (Fig. 3a, b). This suggested that SHIV-infected animals develop villous atrophy, irrespective of viral load.

Increased number of activated macrophages in the jejunum of symptomatic animals

Macrophages appeared to be more abundant in H&E-stained jejunal sections in symptomatic animals. This was confirmed by CD68 staining: the frequency of $CD68^+$ macrophages in the jejunum was considerably higher in symptomatic animals than in uninfected animals, but was not significantly different between uninfected animals and Asym LVL macaques (data not shown). Furthermore, $CD68^+$ macrophages in the small intestine of Sym LVL and HVL macaques appeared to be activated because their size was increased. To examine whether the number of activated $CD68^+$ macrophages increased in the small intestine, we double stained for CD68 and Ki67 in the small intestine sections by immunohistochemistry. The frequency of $CD68^+$ $Ki67^+$ macrophages in the jejunum of all symptomatic animals examined was significantly higher than that of uninfected animals ($P<0.0001$) (Fig. 3c, d). This suggested that abnormal activation of intestinal macrophages occurred in symptomatic animals irrespective of viral load.

DISCUSSION

It is important to discuss initially why some SHIV-infected macaques had an HVL at the late stage, whilst others had

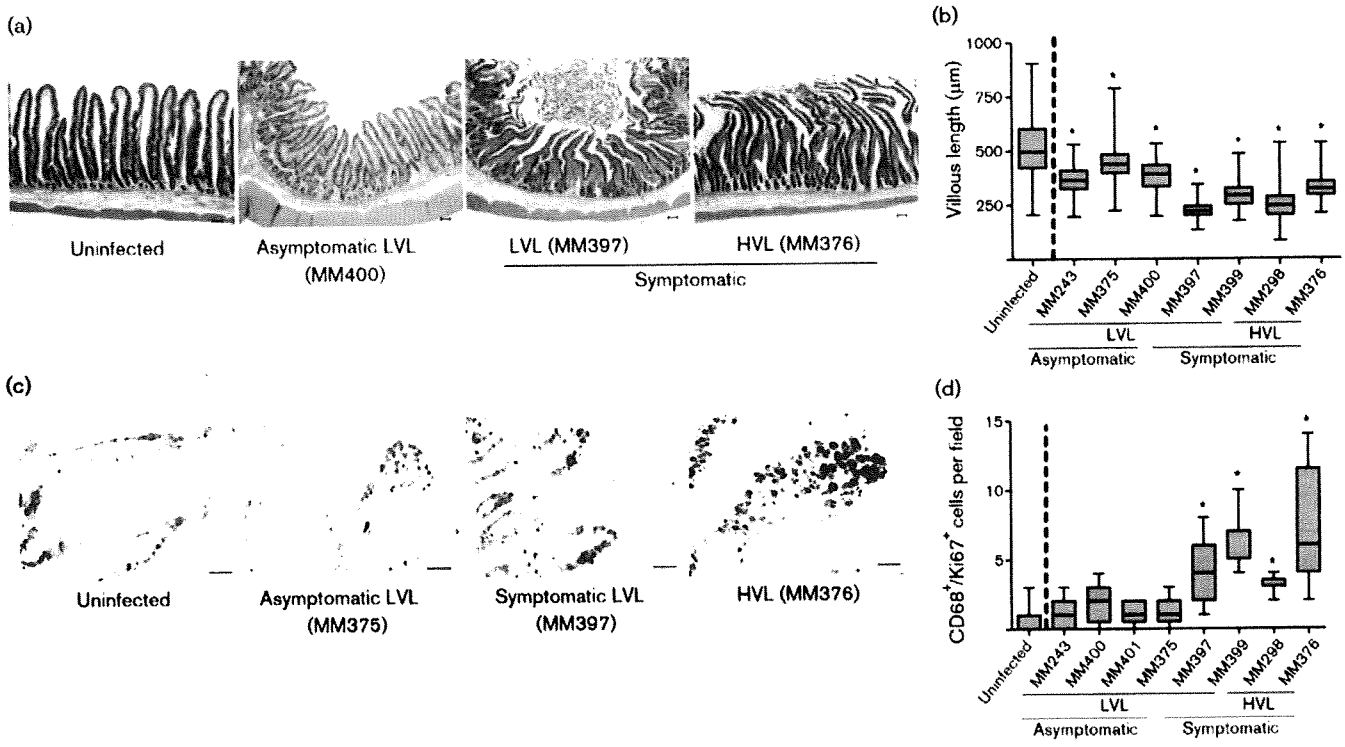

Fig. 3. Villous length in jejunum and counts of activated macrophages in the small intestine at the time of euthanasia in SHIV-KS661-infected rhesus macaques. (a) H&E-stained sections of jejunum of representative uninfected, Asym LVL, Sym LVL and HVL macaques. Bars, 200 μm. (b) Comparison of villous length in uninfected and infected macaques. The lengths of at least 100 villi were measured in each macaque. Statistical analysis was performed using Student's *t*-test for the data from four uninfected and each infected macaque (*, $P<0.0001$). Data for MM299, MM338, MM339 and MM401 were not available. (c) Ki67 and CD68 staining in the small intestine of representative uninfected, Asym LVL, Sym LVL and HVL macaques. Brown staining indicates $Ki67^+$ cells and blue staining indicates $CD68^+$ cells. Bar, 50 μm. (d) Comparison of $CD68^+$ $Ki67^+$ cell counts in uninfected and infected macaques. The numbers of $CD68^+$ $Ki67^+$ cells were enumerated in at least ten fields of the tissues at a magnification of 200×. Statistical analysis was performed using Student's *t*-test for the data from seven uninfected and each infected macaque (*, $P<0.0001$). Data for MM299, MM338 and MM339 were not available.

an LVL. The LVL macaques had much stronger antibody responses than the HVL macaques (Table 1). SHIV-89.6P is easily controlled by the antibody response (Montefiori *et al.*, 1998). SHIV-KS661, which shares its genetic origin with SHIV-89.6P, might be strongly affected by the antibody response. Virus replication during the primary phase clearly occurred later in the intrarectally inoculated macaques than in the intravenously inoculated macaques. Therefore, this delay might contribute to the continuous and strong antibody response in the intrarectally inoculated macaques, consequently resulting in a low viral load in most of the intrarectally inoculated macaques.

The purpose of this study was to elucidate why LVL macaques experience diarrhoea and wasting. A comparison of circulating $CD4^+$ T-cell counts (Fig. 2a) and relative levels of naïve T-cells (Fig. 2b) in LVL macaques did not reveal a substantial difference between Sym LVL (which showed diarrhoea and wasting) and Asym LVL (which were healthy) macaques. The villous length in the intestine also did not affect the level of malignancy of the disease condition, as all infected monkeys showed significant villous atrophy, suggesting a high sensitivity to infection itself. However, Sym LVL and HVL macaques exhibited two findings that Asym LVL macaques did not: (i) $CD4^+$ cell reduction in intestinal and lymphoid tissues (Fig. 2c, d), a hallmark of AIDS; and (ii) abnormal innate immune activation, which was reflected by an increased number of activated macrophages within the intestines (Fig. 3c, d). Ki67 serves as a proliferation marker and proliferation of macrophages may seem unlikely. However, there are some reports about local macrophage proliferation in inflammation sites, indicating the infiltration of activated macrophages associated with tissue damage (Isbel *et al.*, 2001; Norton, 1999). These observations indicated the existence of immunopathological disorders in the intestines not only in HVL macaques but also in Sym LVL macaques.

Many studies have shown positive correlations between the development of AIDS and some characteristic features in

the intestinal tracts of HIV-1-infected humans and pathogenic SIV- or SHIV-infected monkeys: continuous $CD4^+$ T-cell depletion (Brenchley *et al.*, 2004; Ling *et al.*, 2007), abnormal and chronic immune activation (Brenchley *et al.*, 2006; Hazenberg *et al.*, 2003) and enteropathy (Kotler, 2005). Immune activation (as shown by an increased number of intestinal activated macrophages) and intestinal $CD4^+$ cell depletion in Sym LVL macaques strongly suggest the presence of an AIDS-like disease in this subset of animals. Hence, these results suggest that an AIDS-like intestinal disease can occur in LVL macaques despite their low viral load, as well as in HVL macaques.

Some HIV-1-infected patients experience poor recovery of circulating $CD4^+$ T cells, even when their plasma HIV-1 RNA load is suppressed by HAART (Kaufmann *et al.*, 2003; Marchetti *et al.*, 2006; Piketty *et al.*, 1998). These individuals are called immunological non-responders (Marchetti *et al.*, 2006), and have been found to have increased plasma lipopolysaccharide levels, suggesting that bacteria had been translocated from the intestines into the circulation with concomitant activation of T-cell compartments (Marchetti *et al.*, 2006, 2008). Furthermore, some patients who maintain an undetectable or nearly undetectable plasma viral RNA load in the absence of HAART also develop AIDS disease progression (Madec *et al.*, 2005) and have abnormal immune activation and increased plasma lipopolysaccharide levels (Hunt *et al.*, 2008). These observations may indicate that disease progression in a subset of HIV-1-infected individuals is independent of viraemia. Accordingly, the disease progression under conditions of low viral load that we observed in SHIV-KS661-infected macaques can also occur in HIV-1-infected individuals.

Consistent with the fact that intestinal $CD4^+$ cell depletion triggers mucosal immune dysfunction, a notable difference observed between Sym LVL and Asym LVL macaques was the low $CD4^+$ cell frequency in the intestines of the Sym LVL macaques. We propose that the intestinal $CD4^+$ cells in Sym LVL macaques were not able to recover after intestinal $CD4^+$ cell reduction during the early phases of infection. We reported previously that SHIV-KS661 infection of rhesus macaques caused early intestinal $CD4^+$ T-cell depletion (Fukazawa *et al.*, 2008; Miyake *et al.*, 2006). Although we did not examine the macaques during the early phases of infection, the intestinal $CD4^+$ T cells of both Sym LVL and Asym LVL macaques should have been depleted at this time, as even moderately pathogenic SHIV can cause intestinal $CD4^+$ cell reduction during the early phase of infection (Fukazawa *et al.*, 2008). Therefore, the near-normal frequency of intestinal $CD4^+$ cells in Asym LVL macaques would be the result of $CD4^+$ cell recovery after intestinal $CD4^+$ cell reduction during the early phase of infection. In contrast, intestinal $CD4^+$ cells in Sym LVL macaques may be unable to recover, even though virus replication has been controlled. Similarly, intestinal $CD4^+$ cell recovery was found to be important for halting disease progression in SIVmac239-infected rhesus macaques (Ling *et al.*, 2007). Accordingly, one of the important determinants for disease progression in SHIV-KS661-infected macaques may be $CD4^+$ cell recovery in the intestines.

We further hypothesize that this inappropriately low level of $CD4^+$ cells within the intestines of the SHIV-KS661-infected animals (and phenotypically similar humans) is permissive to the excessive activation of resident tissue macrophages. One implication of these studies is that regulatory T-cell subsets of $CD4^+$ cells may be especially vulnerable to this depletion, thus allowing this macrophage activation in view of the well-known role of regulatory T cells in inhibiting innate immune responses (Maloy *et al.*, 2003). This hypothesis will be important to assess in future studies to understand the pathophysiology in the intestines during the chronic phase of HIV-1 infection.

Taken together, the present results suggest that $CD4^+$ cell reduction and enteropathy can occur in SHIV-KS661-infected rhesus macaques even when the viral load is low. The ability or inability to restore intestinal $CD4^+$ cells may be a key factor determining disease progression, irrespective of virus replication levels in the chronic phase of SHIV-KS661 infection. The reason that the recovery of intestinal $CD4^+$ cells is impeded is unknown, although we can speculate on some possibilities such as the co-existence of other infectious microbial agents or impaired T-cell reconstitution caused by damage during thymopoiesis at an early phase of SHIV infection (Motohara *et al.*, 2006). We demonstrated comparable proviral DNA loads in the examined tissues between Sym and Asym LVL macaques, although the $CD4^+$ cell frequencies in the tissues were clearly reduced in Sym LVL macaques. Therefore, the quantity of provirus per CD4 cell in the tissues of Sym LVL macaques is considered to be relatively higher than that of Asym LVL macaques, and low-level replication that may be undetectable in the plasma viral load might be maintained in Sym LVL but not in Asym LVL macaques. Identifying the mechanisms of poor recovery of intestinal $CD4^+$ cells is needed to understand AIDS pathogenesis, because, as stated above, some HIV-1-infected patients have low $CD4^+$ T-cell counts even when viraemia is controlled. One useful approach is comparative and periodical analysis, including cellular immunology data, of the intestinal tract of the same animals from the early to the chronic phases using Sym LVL and Asym LVL macaques in this SHIV infection macaque model.

METHODS

Virus, animals and sample collection. Highly pathogenic SHIV-KS661 is a molecular clone of SHIV-C2/1 (GenBank accession no. AF217181), which was derived through *in vivo* passages of SHIV-89.6 (Shinohara *et al.*, 1999). The virus stock was prepared from the supernatant of virus-infected CEMx174 and M8166 human lymphoid cell lines.

All rhesus macaques used in this study were treated in accordance with the institutional regulations approved by the Committee for

Experimental Use of Non-human Primates in the Institute for Virus Research, Kyoto University, Japan. All macaques were inoculated with 2×10^3 50 % tissue culture infectious dose of SHIV-KS661 measured with CEMx174. The animal ID numbers, infection route and when they were euthanized are provided in Fig. 1(a).

Blood was collected periodically using sodium citrate as an anti-coagulant and examined by flow cytometry and for quantification of plasma viral RNA load. Tissue samples were obtained at the time of euthanasia and were used for quantification of proviral DNA and histopathology.

Determination of plasma viral RNA and proviral DNA loads. The viral loads in plasma and proviral DNA loads in lymphoid and intestinal tissues were determined by quantitative RT-PCR and quantitative PCR, respectively, as described previously (Motohara *et al.*, 2006). DNA samples were extracted directly from frozen tissue sections of each monkey using a DNeasy Tissue kit (Qiagen) according to the manufacturer's protocol.

Determination of antibody titres. Anti-HIV antibody titres were determined using a commercial particle agglutination kit (Serodia-HIV1/2; Fujirebio). Isolated plasma samples were serially diluted and assayed. The end point of the highest dilution giving a positive result was determined as the titre.

Flow cytometry. Flow cytometry was performed as described previously (Motohara *et al.*, 2006). Briefly, $CD4^+$ T cells were analysed by a combination of fluorescein isothiocyanate (FITC)-conjugated anti-monkey CD3 (clone FN-18; BioSource) and phycoerythrin-conjugated anti-human CD4 (clone NU-TH/I; Nichirei), and subsets of naïve and memory $CD4^+$ cells were analysed by a combination of FITC-conjugated anti-human CD95 (clone DX2; BD Pharmingen) and allophycocyanin-conjugated anti-human CD4 (clone L200; BD Pharmingen). $CD95^-$ $CD4^+$ cells were defined as naïve $CD4^+$ T cells and $CD95^+$ $CD4^+$ cells were defined as memory $CD4^+$ T cells. Labelled lymphocytes were examined on a FACSCalibur analyser using CellQuest software (BD Biosciences).

Histology and immunohistochemistry. Tissue samples were fixed in 4 % paraformaldehyde in PBS at 4 °C overnight and embedded in paraffin wax. Sections (4 μm) were dewaxed using xylene, rehydrated through an alcohol gradient, and stained with H&E. The villous length of the jejunum was measured with a micrometer. At least 40 villi from each section were measured.

For immunohistochemistry, sections were rehydrated and processed for 10 min in an autoclave in 10 mM citrate buffer (pH 6.0) to unmask the antigens, sequentially treated with TBS/Tween 20 (TBST) and aqueous hydrogen peroxide, left at 4 °C overnight or at room temperature for 30 min or 1 h for primary antibody reactions, washed with TBST, incubated at room temperature for 1 h with an Envision+ kit (a horseradish peroxidase-labelled anti-mouse immunoglobulin polymer; Dako), visualized using diaminobenzidine (DAB) substrate (Dako) as a chromogen, rinsed in distilled water, counterstained with haematoxylin and analysed by light microscopy (Biozero BZ-8000: Keyence).

For double staining (CD68 and Ki67) of sections, appropriately processed sections were incubated at room temperature for 1 h with unlabelled anti-Ki67 antibody at a dilution of 1:2000, the highly sensitive tyramide amplification step (CSAII; Dako) was performed, the slides were reacted with DAB to visualize the results and incubated with unlabelled anti-CD68 antibody at 4 °C overnight followed by incubation at room temperature for 1 h with Histofine Simple Stain AP (an alkaline phosphatase-labelled anti-mouse immunoglobulin polymer (Nichirei), and the results were visualized with a Blue Alkaline Phosphatase Substrate kit III (Vector Laboratories). Measurements of $CD68^+$ $Ki67^+$ cell counts were performed in ten fields at a magnification of 200 × by light microscopy.

Primary antibodies used in immunohistochemistry were anti-human CD4 (diluted 1:30; clone NCL-CD4; Novacastra Laboratories), anti-SIV Nef (diluted 1:500; FIT Biotech), anti-human CD68 (diluted 1:50; clone KP-1; Dako) and anti-human Ki67 (Ki-S5; Dako).

Statistical analysis. The significance of $CD4^+$ or $CD68^+$ $Ki67^+$ cell frequency measurements and villous length in the jejunum of infected monkeys compared with uninfected monkeys was analysed using an unpaired Student's *t*-test (two-tailed) using GraphPad Prism 4.0E software (Varsity Wave).

ACKNOWLEDGEMENTS

We are grateful to Dr James Raymond for editing the English of this manuscript; to Takahito Kazama, Reii Horiuchi, Noriko Nakajima and Tetsutaro Sata for technical support; to Dr Michael A. Eckhaus for histopathological interpretation; and to Takeshi Kobayashi for critical reading. This work was supported, in part, by Research on HIV/AIDS in Health and Labour Sciences Research Grants from the Ministry of Health, Labour and Welfare, Japan; a Grant-in-Aid for Scientific Research from the Ministry of Education and Science, Japan; a Research Grant for AIDS on Health Sciences focusing on Drug Innovation from the Japan Health Sciences Foundation; and a Program for the Promotion of Fundamental Studies in Health Sciences of the National Institute of Biomedical Innovation (NIBIO) of Japan.

REFERENCES

Anton, P. A., Elliott, J., Poles, M. A., McGowan, I. M., Matud, J., Hultin, L. E., Grovit-Ferbas, K., Mackay, C. R., Chen, I. S. Y. & Giorgi, J. V. (2000). Enhanced levels of functional HIV-1 co-receptors on human mucosal T cells demonstrated using intestinal biopsy tissue. *AIDS* **14**, 1761–1765.

Batman, P. A., Miller, A. R., Forster, S. M., Harris, J. R., Pinching, A. J. & Griffin, G. E. (1989). Jejunal enteropathy associated with human immunodeficiency virus infection: quantitative histology. *J Clin Pathol* **42**, 275–281.

Brenchley, J. M., Schacker, T. W., Ruff, L. E., Price, D. A., Taylor, J. H., Beilman, G. J., Nguyen, P. L., Khoruts, A., Larson, M. & other authors (2004). $CD4^+$ T cell depletion during all stages of HIV disease occurs predominantly in the gastrointestinal tract. *J Exp Med* **200**, 749–759.

Brenchley, J. M., Price, D. A., Schacker, T. W., Asher, T. E., Silvestri, G., Rao, S., Kazzaz, Z., Bornstein, E., Lambotte, O. & other authors (2006). Microbial translocation is a cause of systemic immune activation in chronic HIV infection. *Nat Med* **12**, 1365–1371.

Fackler, O. T., Schafer, M., Schmidt, W., Zippel, T., Heise, W., Schneider, T., Zeitz, M., Riecken, E. O., Mueller-Lantzsch, N. & Ullrich, R. (1998). HIV-1 p24 but not proviral load is increased in the intestinal mucosa compared with the peripheral blood in HIV-infected patients. *AIDS* **12**, 139–146.

Fukazawa, Y., Miyake, A., Ibuki, K., Inaba, K., Saito, N., Motohara, M., Horiuchi, R., Himeno, A., Matsuda, K. & other authors (2008). Small intestine $CD4^+$ T cells are profoundly depleted during acute simian–human immunodeficiency virus infection, regardless of viral pathogenicity. *J Virol* **82**, 6039–6044.

Gibbons, T. & Fuchs, G. J. (2007). Chronic enteropathy: clinical aspects. *Nestle Nutr Workshop Ser Pediatr Program* **59**, 89–101.

Hazenberg, M. D., Otto, S. A., van Benthem, B. H., Roos, M. T., Coutinho, R. A., Lange, J. M., Hamann, D., Prins, M. & Miedema, F.

(2003). Persistent immune activation in HIV-1 infection is associated with progression to AIDS. *AIDS* **17**, 1881–1888.

Hunt, P. W., Brenchley, J., Sinclair, E., McCune, J. M., Roland, M., Page-Shafer, K., Hsue, P., Emu, B., Krone, M. & other authors (2008). Relationship between T cell activation and $CD4^+$ T cell count in HIV-seropositive individuals with undetectable plasma HIV RNA levels in the absence of therapy. *J Infect Dis* **197**, 126–133.

Isbel, N. M., Nikolic-Paterson, D. J., Hill, P. A., Dowling, J. & Atkins, R. C. (2001). Local macrophage proliferation correlates with increased renal M-CSF expression in human glomerulonephritis. *Nephrol Dial Transplant* **16**, 1638–1647.

Kahn, E. (1997). Gastrointestinal manifestations in pediatric AIDS. *Pediatr Pathol Lab Med* **17**, 171–208.

Kaufmann, G. R., Perrin, L., Pantaleo, G., Opravil, M., Furrer, H., Telenti, A., Hirschel, B., Ledergerber, B., Vernazza, P. & other authors (2003). CD4 T-lymphocyte recovery in individuals with advanced HIV-1 infection receiving potent antiretroviral therapy for 4 years: the Swiss HIV Cohort Study. *Arch Intern Med* **163**, 2187–2195.

Kotler, D. P. (2005). HIV infection and the gastrointestinal tract. *AIDS* **19**, 107–117.

Lapenta, C., Boirivant, M., Marini, M., Santini, S. M., Logozzi, M., Viora, M., Belardelli, F. & Fais, S. (1999). Human intestinal lamina propria lymphocytes are naturally permissive to HIV-1 infection. *Eur J Immunol* **29**, 1202–1208.

Ling, B., Veazey, R. S., Hart, M., Lackner, A. A., Kuroda, M., Pahar, B. & Marx, P. A. (2007). Early restoration of mucosal CD4 memory CCR5 T cells in the gut of SIV-infected rhesus predicts long term non-progression. *AIDS* **21**, 2377–2385.

Madec, Y., Boufassa, F., Porter, K. & Meyer, L. (2005). Spontaneous control of viral load and CD4 cell count progression among HIV-1 seroconverters. *AIDS* **19**, 2001–2007.

Maloy, K. J., Salaun, L., Cahill, R., Dougan, G., Saunders, N. J. & Powrie, F. (2003). $CD4^+CD25^+$ T_R cells suppress innate immune pathology through cytokine-dependent mechanisms. *J Exp Med* **197**, 111–119.

Marchetti, G., Gori, A., Casabianca, A., Magnani, M., Franzetti, F., Clerici, M., Perno, C. F., Monforte, A., Galli, M. & Meroni, L. (2006). Comparative analysis of T-cell turnover and homeostatic parameters in HIV-infected patients with discordant immune-virological responses to HAART. *AIDS* **20**, 1727–1736.

Marchetti, G., Bellistri, G. M., Borghi, E., Tincati, C., Ferramosca, S., La Francesca, M., Morace, G., Gori, A. & Monforte, A. D. (2008). Microbial translocation is associated with sustained failure in $CD4^+$ T-cell reconstitution in HIV-infected patients on long-term highly active antiretroviral therapy. *AIDS* **22**, 2035–2038.

Miyake, A., Ibuki, K., Enose, Y., Suzuki, H., Horiuchi, R., Motohara, M., Saito, N., Nakasone, T., Honda, M. & other authors (2006). Rapid dissemination of a pathogenic simian/human immunodeficiency virus to systemic organs and active replication in lymphoid tissues following intrarectal infection. *J Gen Virol* **87**, 1311–1320.

Montefiori, D. C., Reimann, K. A., Wyand, M. S., Manson, K., Lewis, M. G., Collman, R. G., Sodroski, J. G., Bolognesi, D. P. & Letvin, N. L. (1998). Neutralizing antibodies in sera from macaques infected with chimeric simian–human immunodeficiency virus containing the envelope glycoproteins of either a laboratory-adapted variant or a primary isolate of human immunodeficiency virus type 1. *J Virol* **72**, 3427–3431.

Motohara, M., Ibuki, K., Miyake, A., Fukazawa, Y., Inaba, K., Suzuki, H., Masuda, K., Minato, N., Kawamoto, H. & other authors (2006). Impaired T-cell differentiation in the thymus at the early stages of acute pathogenic chimeric simian–human immunodeficiency virus (SHIV) infection in contrast to less pathogenic SHIV infection. *Microbes Infect* **8**, 1539–1549.

Norton, W. T. (1999). Cell reactions following acute brain injury: a review. *Neurochem Res* **24**, 213–218.

Paiardini, M., Frank, I., Pandrea, I., Apetrei, C. & Silvestri, G. (2008). Mucosal immune dysfunction in AIDS pathogenesis. *AIDS Rev* **10**, 36–46.

Piketty, C., Castiel, P., Belec, L., Batisse, D., Si Mohamed, A., Gilquin, J., Gonzalez-Canali, G., Jayle, D., Karmochkine, M. & other authors (1998). Discrepant responses to triple combination antiretroviral therapy in advanced HIV disease. *AIDS* **12**, 745–750.

Sestak, K. (2005). Chronic diarrhea and AIDS: insights into studies with non-human primates. *Curr HIV Res* **3**, 199–205.

Sharpstone, D. & Gazzard, B. (1996). Gastrointestinal manifestations of HIV infection. *Lancet* **348**, 379–383.

Shinohara, K., Sakai, K., Ando, S., Ami, Y., Yoshino, N., Takahashi, E., Someya, K., Suzaki, Y., Nakasone, T. & other authors (1999). A highly pathogenic simian/human immunodeficiency virus with genetic changes in cynomolgus monkey. *J Gen Virol* **80**, 1231–1240.

Smith, P. D., Meng, G., Salazar-Gonzalez, J. F. & Shaw, G. M. (2003). Macrophage HIV-1 infection and the gastrointestinal tract reservoir. *J Leukoc Biol* **74**, 642–649.

Veazey, R. S., DeMaria, M., Chalifoux, L. V., Shvetz, D. E., Pauley, D. R., Knight, H. L., Rosenzweig, M., Johnson, R. P., Desrosiers, R. C. & Lackner, A. A. (1998). Gastrointestinal tract as a major site of $CD4^+$ T cell depletion and viral replication in SIV infection. *Science* **280**, 427–431.

Veazey, R. S., Mansfield, K. G., Tham, I. C., Carville, A. C., Shvetz, D. E., Forand, A. E. & Lackner, A. A. (2000a). Dynamics of CCR5 expression by $CD4^+$ T cells in lymphoid tissues during simian immunodeficiency virus infection. *J Virol* **74**, 11001–11007.

Veazey, R. S., Tham, I. C., Mansfield, K. G., DeMaria, M., Forand, A. E., Shvetz, D. E., Chalifoux, L. V., Sehgal, P. K. & Lackner, A. A. (2000b). Identifying the target cell in primary simian immunodeficiency virus (SIV) infection: highly activated memory $CD4^+$ T cells are rapidly eliminated in early SIV infection in vivo. *J Virol* **74**, 57–64.

Wilcox, C. M. & Saag, M. S. (2008). Gastrointestinal complications of HIV infection: changing priorities in the HAART era. *Gut* **57**, 861–870.

Virology 386 (2009) 23–31

Contents lists available at ScienceDirect

Virology

journal homepage: www.elsevier.com/locate/yviro

Raft localization of CXCR4 is primarily required for X4-tropic human immunodeficiency virus type 1 infection

Haruka Kamiyama [a,b], Hiroaki Yoshii [a], Yuetsu Tanaka [c], Hironori Sato [a,d], Naoki Yamamoto [a,e], Yoshinao Kubo [a,*]

[a] Department of AIDS Research, Institute of Tropical Medicine, Nagasaki University, 1-12-4 Sakamoto, Nagasaki, Nagasaki 852-8523, Japan
[b] Department of Cellular Biochemistry, Graduate School of Human Health Science, Siebold University of Nagasaki, Nagayo, Nagasaki 851-2195, Japan
[c] Department of Immunology, Graduate School and Faculty of Medicine, University of the Ryukyus, Nishihara, Okinawa 903-0215, Japan
[d] Laboratory of Viral Genomics, Center for Pathogen Genomics, National Institute of Infectious Diseases, Gakuen 4-7-1, Musashimurayama-shi, Tokyo 208-0011, Japan
[e] AIDS Research Center, National Institute of Infectious Diseases, Shinjuku-ku, Tokyo 162-8640, Japan

ARTICLE INFO

Article history:
Received 3 June 2008
Returned to author for revision
10 November 2008
Accepted 17 December 2008

Keywords:
CD4-independent HIV-1
CXCR4
Raft

ABSTRACT

Human immunodeficiency virus type 1 (HIV-1) infection is initiated by successive interactions of viral envelope glycoprotein gp120 with two cellular surface proteins, CD4 and chemokine receptor. The two most common chemokine receptors that allow HIV-1 entry are the CCR5 and CXCR4. The CD4 and CCR5 are mainly localized to the particular plasma membrane microdomains, termed raft, which is rich in glycolipids and cholesterol. However, the CXCR4 is localized only partially to the raft region. Although the raft domain is suggested to participate in HIV-1 infection, its role in entry of CXCR4-tropic (X4-tropic) virus is still unclear. Here, we used a combination of CD4-independent infection system and cholesterol-depletion-inducing reagent, methyl-β-cyclodextrin (MβCD), to address the requirement of raft domain in the X4-tropic virus infection. Treatment of CD4-negative, CXCR4-positive human cells with MβCD inhibited CD4-independent infection of the X4-tropic strains. This inhibitory effect of the cholesterol depletion was observed even when the CXCR4 was over-expressed on the target cells. Soluble CD4-induced infection was also inhibited by MβCD. The MβCD had no effect on the levels of cell surface expression of CXCR4. In contrast to these infections, MβCD treatment did not inhibit CD4-dependent HIV-1 infection in the wild type CD4-expressing cells. This study and previous reports showing that CD4 mutants localized to non-raft domains function as HIV-1 receptor indicate that CXCR4 clustering in the raft microdomains, rather than CD4, is the key step for the HIV-1 entry.

© 2008 Elsevier Inc. All rights reserved.

Introduction

Human immunodeficiency virus type 1 (HIV-1) gains entry into susceptible cells by fusion of the viral membrane with the cell plasma membrane (Dimitrov, 2000). This process is generally initiated by the binding of the HIV-1 envelope (Env) glycoprotein gp120 to CD4 on the host cell surface. The binding then induces conformational change of the gp120, which allows gp120 to interact with a cellular surface chemokine receptor, termed coreceptor. HIV-1 can use many types of chemokine receptors for the entry (Shimizu et al., 2000). The two most common types of the coreceptors of the HIV-1 are the CC chemokine receptor 5 (CCR5) and the CXC chemokine receptor 4 (CXCR4) (Berger et al., 1999). Successive conformational changes in the gp120 during these interactions with cellular surface molecules render initially occluded hydrophobic domain of the envelope gp41 subunit available to fusion with cellular plasma membrane (Doms, 2000).

Clustering of multiple CD4 and coreceptor molecules at the site of the fusion is presumed to be necessary for the efficient fusion of the viral and host cell membranes (Kuhmann et al., 2000). Because both the gp120–CD4 and gp120–chemokine receptor associations are reversible, and because CD4 binding site of the gp120 is conformationally masked (Kwong et al., 2002), multiple CD4 and chemokine receptor molecules should almost simultaneously be gathered and interact with the multiple gp120 at the place of virus–host cell membrane fusion (Dimitrov 2000; Doms, 2000; Kwong et al., 2002).

Membrane microdomains or lipid rafts are regions of host cell membrane enriched in glycosphingolipids, sphingomyelin, cholesterol, glycophosphatidylinositol-anchored proteins, and signaling proteins (Simons and Ikonen, 1997). The rafts are thought to serve as sites for recruitment of gp120–gp41–CD4–coreceptor complexes in a limited area on the cell surface. Increasing evidence indicate such a scaffolding role of the rafts in HIV-1 entry; (i) HIV-1 infection is blocked by targeting CD4 to non-raft membrane domains (Del Real et al., 2002); (ii) membrane raft microdomains mediate lateral assemblies required for HIV-1 infection (Manes et al., 2000); (iii) HIV-1 gp120-induced co-clustering of CD4 and coreceptor into the raft

* Corresponding author. Fax: +81 95 819 7805.
E-mail address: yoshinao@net.nagasaki-u.ac.jp (Y. Kubo).

0042-6822/$ - see front matter © 2008 Elsevier Inc. All rights reserved.
doi:10.1016/j.virol.2008.12.033

domains is prevented by removal of cholesterol from cell plasma membrane and the depletion of cholesterol from target cells inhibits their susceptibility to HIV-1 infection (Manes et al., 2000; Popik et al., 2002; Liao et al., 2001; Viard et al., 2002). Together with other results, reported data are compatible with the possibility that the recruitment of gp120–gp41–CD4-coreceptor complexes into the raft domains is required for the HIV-1 infection (Liao et al., 2001; Manes et al., 2000; Popik et al., 2002). However, it is not clear what is the determinant for the recruitment of the complexes into raft domains.

CD4 (Millan et al., 1999; Manes et al., 2000; Del Real et al., 2002) and CCR5 (Nguyen and Taub, 2002b; Gaibelet et al., 2006) have been demonstrated to be present in lipid rafts, and to constitutively interact each other before the gp120 binding. In contrast, CXCR4 is localized only partially to the rafts, as evidenced with partial colocalization with GM1, a raft marker (Manes et al., 2000; Del Real et al., 2002; Nguyen and Taub, 2002a). It has been reported that a CD4 mutant, which is localized to non-raft domains of the plasma membrane, blocks HIV-1 entry, indicating that raft localization of CD4 is critical in HIV-1 infection (Del Real et al., 2002). However, more recent studies are consistent with a possibility that the raft localization of CD4 is not required for the virus entry (Popik and Alce, 2004; Percherancier et al., 2003), indicating that CD4 is not the determinant for clustering of gp120–gp41–CD4–chemokine receptor complexes into raft domains. Due to the initial localization of CXCR4 in the non-raft region and the inconsistencies in prior studies, a role of raft domains in CXCR4-tropic (X4-tropic) HIV-1 entry is not clear yet.

These apparently controversial observations prompted us to examine the possibility that recruitment of CXCR4 to raft microdomains, rather than CD4 raft localization, is the determinant for the clustering of gp120–gp41–CD4–CXCR4 complexes into raft domains. To test the possibility, we used HIV-1 pseudotype viruses that have the X4-tropic Env proteins and can establish infection of CXCR4-expressing cells without interaction with CD4 (CD4-independent infection). The viruses were used to infect cells whose cholesterol were depleted in advance with treatment by a cholesterol-solubilizing agent, methyl-β-cyclodextrin (MβCD) (Simons and Ikonen, 1997), and viral infectivity was measured. We further examined a role of raft localization of CXCR4 in the HIV-1 entry, as follows. The CD4-dependent infection induced by soluble CD4 was used to infect cholesterol-depleted cells. By this approach, we can determine if the raft localization of CXCR4 is essential in the HIV-1 infections, because these infections occur independently of CD4 raft localization. Our results are compatible with the working hypothesis described above and suggest a supportive role of CD4 in augmenting the raft recruitment/clustering of CXCR4.

Results

MβCD inhibits CD4-independent, CXCR4-dependent HIV-1 infection

To examine whether raft domain architectures are required for CD4-dependent and -independent entry of X4-tropic viruses, we used an infection system of pseudotyped viruses carrying Env proteins of X4-tropic HIV-1 strains, mNDK, or 8X, that allow both CD4-dependent and -independent infections in CD4-positive and -negative cells, respectively (Dumonceaux et al., 1998, Hoffman et al., 1999, Kubo et al., 2007). As targets of virus infections, we used human NP2 cells expressing both CD4 and CXCR4, or CXCR4 alone (Soda et al., 1999). The raft domain of target cells were depleted by the treatment with MβCD (Simons and Ikonen, 1997) and used for infections of the pseudotyped HIV-1 viruses. As a control of HIV-1 receptor independent infection, we used the VSV-G-pseudotyped HIV-1. Incubation with MβCD did not suppress but rather increased the VSV-G-pseudotyped virus infection (Fig. 1A). This MβCD treatment (1 and 5 mM) did not affect cell growth (data not shown).

Notably, transduction titers of the HIV-1 vectors having the CD4-independent Env proteins (mNDK and 8X) were reduced to about 25% by the increasing concentrations of MβCD treatments of the CD4-negative, CXCR4-positive cells (Fig. 1B, gray bars, NP2/X4 cells). In contrast, inhibitory effects of MβCD were less prominent in the CD4-dependent infections of the same viruses: transduction titers of the HIV-1 vectors were reduced to about 75% at 5 mM of MβCD (Fig. 1B, open bars, NP2/CD4/X4 cells). Transduction titer of the HIV-1 vector having Env protein of the NDK HIV-1 strain, the CD4-dependent parental strain of the mNDK variant, was not significantly inhibited by MβCD (Fig. 1C). These results show that MβCD inhibits CXCR4-mediated infection but co-expression of CD4 counteracts the inhibitory effects. When excess of cholesterol was added, the inhibitory effect of MβCD on the CD4-independent infection was abrogated (Fig. 1D), confirming that cholesterol extraction is a primary cause of suppression of the CD4-independent infection by MβCD.

To assess if the MβCD treatment indeed had depleted cholesterol from target cell membranes, cells were stained with the cholesterol-binding agent, filipin. Binding of filipin to cholesterol decreases filipin fluorescence at 525 nm (Severs and Robenek, 1983; Castanho et al., 1992). Fluorescence strength of filipin in the MβCD-treated cells was reproductively increased compared to that of the untreated control cells (Fig. 1E). The results indicate that cholesterol of cell membrane was indeed extracted by MβCD treatment in our experimental system.

Over-expression of CXCR4 does not affect the inhibitory effect of MβCD on CD4-independent HIV-1 infection

In our CD4-independent infection system, virus enters into cells using endogeneously expressed CXCR4. To know whether MβCD still inhibits infection when cells express exogenously abundant amounts of CXCR4, human 293T and TE671 cells were transduced by an HA-tagged CXCR4 encoding murine leukemia virus vector (Kubo et al., 2003). Over-expression of CXCR4 in the transduced cells was observed by flow cytometry analysis (Fig. 2A). Transduction titers of the CD4-independent mNDK vector in the CXCR4-over-expressing cells increased about 3 to 4 times compared to those in the original cells (Fig. 2B). This result indicates that CXCR4-over-expression increases the susceptibility to CD4-independent infection.

Effect of CXCR4-over-expression on the inhibition of CD4-independent infection by MβCD was analyzed. The MβCD treatment suppressed the CD4-independent infection in the CXCR4-over-expressing cells, as it did in the original cells (Fig. 3, upper 4 panels). However, exogenous introduction of CD4 into the target cells abrogated the inhibitory effect of MβCD on the HIV-1 infection (Fig. 3 lower panel), as reported (Viard et al., 2002). The results indicate that maintenance of the raft domain architectures on the plasma membrane of the target cells are absolutely required for the CD4-independent infection and suggest that the raft localization of CXCR4 is important for the HIV-1 entry. The treatment with MβCD alone or MβCD plus cholesterol occasionally conferred transduction titers of the VSV-G and mNDK vectors higher (Figs. 1A, D, and 3). The mechanism was not understood.

MβCD treatment inhibits CD4-independent HIV-1 Env-mediated cell-cell fusion

The above result showed that the depletion of cholesterol by MβCD inhibited the HIV-1 Env-mediated infection. To examine if the depletion of cholesterol affects the HIV-1 Env-mediated cell-cell fusion, Env expression plasmid-transfected effector cells and LTR-LacZ-transfected target cells were co-cultured (see Materials and methods). The target cells were co-transfected with the Tat expression and LTR-LacZ plasmids, and then were treated with MβCD. LacZ activities of the cells were comparable between the cells with and without

the MβCD treatment (data not shown), indicating that the MβCD treatment does not affect LacZ functional expression. In NP2/CD4/X4 cells, the mNDK Env-mediated cell-cell fusion was not significantly inhibited by MβCD (Fig. 4, NP2/CD4/X4). On the other hand, in CD4-negative NP2/X4, TE671, and 293T cells, the CD4-independent mNDK Env-mediated cell–cell fusion was inhibited to 40 to 60% of that in the untreated cells (Fig. 4, NP2/X4, TE671, and 293 T). The results are consistent with previous study (Ablan et al., 2006). The cell–cell fusion activity inhibited by MβCD was recovered, when excess of cholesterol was added into the culture (Fig. 4, MβCD+chol). The results were compatible with those of cell-free virus infection (Figs. 1 and 3). Taken together, our results suggest that cholesterol in the cell membrane played an important role in the CD4-independent HIV-1 Env-induced cell–cell fusion and virus entry.

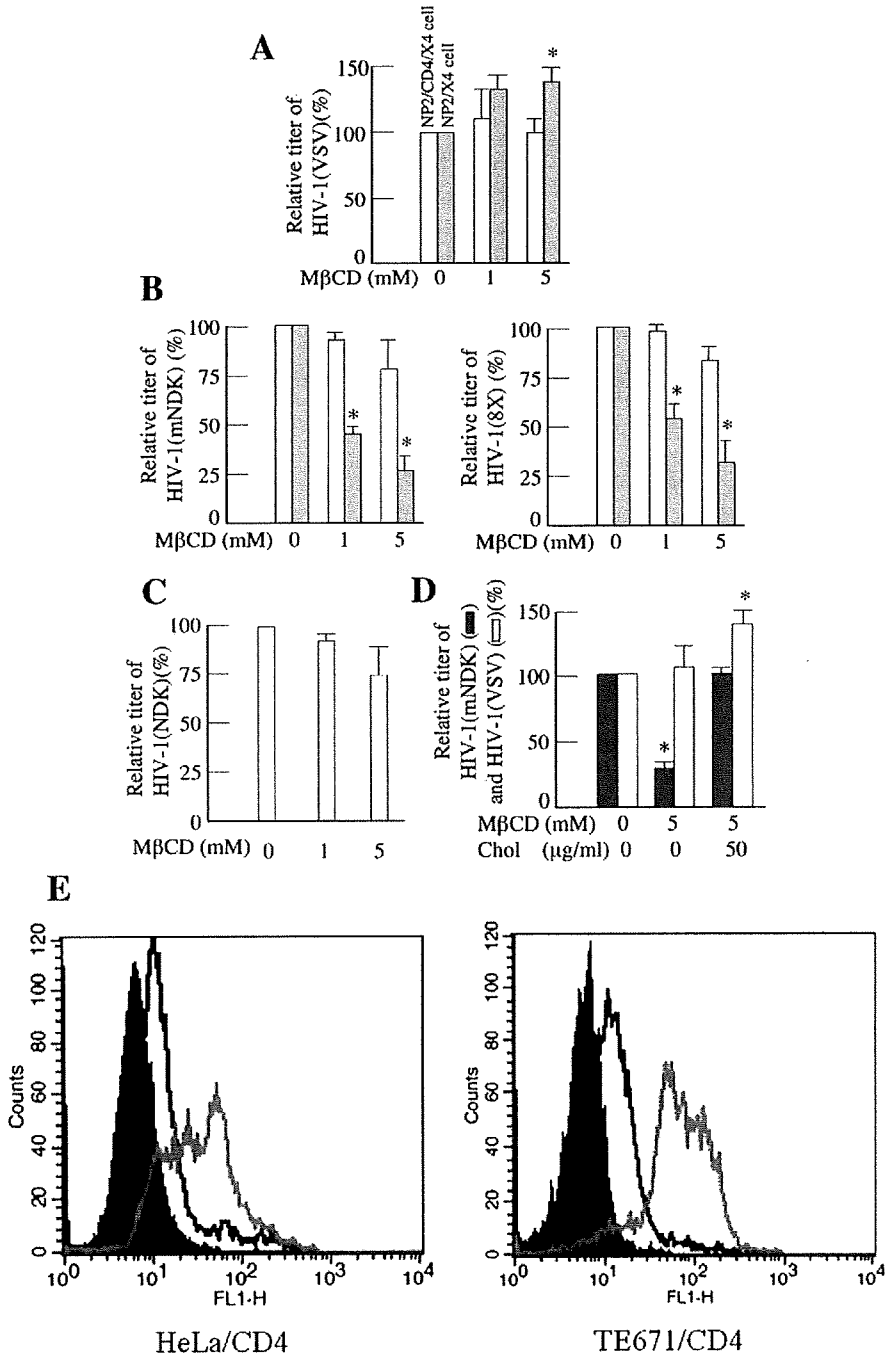

Fig. 1. Effects of MβCD on HIV-1 infection by different Env protein. (A) Effects of MβCD on VSV-G-pseudotyped vector infection in NP2 cells expressing CXCR4 alone (NP2/X4) or both of CXCR4 and CD4 (NP2/CD4/X4). Cells were treated with 0, 1, 5 mM MβCD for 30 min at 37 °C. (B) Effects of MβCD on CD4-independent mNDK Env-pseudotyped HIV-1 vector infection in NP2/X4 and NP2/CD4/X4 cells. Cells were treated with 0, 1, 5 mM MβCD for 30 min at 37 °C. (C) Effects of MβCD on the CD4-dependent NDK-pseudotyped vector in NP2/CD4/X4 cells. (D) Abrogation of MβCD inhibitory effects on mNDK vector infection by cholesterol. The cells were pre-treated for 30 min at 37 °C as indicated. Relative transduction titers to those in untreated cells are indicated. This experiment was repeated three times and results are shown as means+SD. Asterisks indicate statistically significant differences compared to their controls. (E) Cholesterol levels in HeLa/CD4 or TE671/CD4 cells after MβCD treatment. MβCD-treated cells were stained with filipin, and fluorescence strength at 525 nm was analyzed by a flow cytometer. Closed area indicates cells unstained with filipin as a negative control. Open area indicates MβCD-untreated and filipin-stained cells. Gray lines indicate MβCD-treated and filipin-stained cells.

To assess the possibility that MβCD altered the CXCR4 expression, expression levels of CXCR4 in the treated cells were analyzed by a flow cytometer. Treatment of MβCD did not affect the expression of CXCR4 in NP2/X4, 293 T, and TE671 cells (Fig. 5). This result indicates that the inhibition of CD4-independent infection by MβCD is not induced by reducing CXCR4 expression.

Localization of CXCR4 in rafts

The classical way to examine the raft association of membrane proteins includes treatment of cells with Triton X-100 followed by Western blot analysis of soluble and insoluble fractions. The fractions that are not solubilized by Triton X-100 are defined as the raft membrane domains (Simons and Ikonen, 1997). Using this approach, we examined localization of CXCR4 in the raft domains in the presence or absence of MβCD. We also examined raft localization of CD4 as a maker of raft protein (Manes et al., 2000; Del Real et al., 2002; Percherancier et al., 2003; Popik and Alce, 2004). CD4 levels in the insoluble fraction were higher than that in the soluble fraction in all cells examined (Fig. 6A), suggesting that raft domains were correctly separated by this protocol. In contrast to CD4, CXCR4 levels in the insoluble fractions of NP2 and TE671 cells were lower than those in the soluble fractions. In contrast to these cells, CXCR4 was detected in the insoluble fraction of 293T cells. CXCR4 was detected in both of soluble and insoluble fractions after treatment of 293T cells with MβCD (Fig. 6A), suggesting that CXCR4 is partially transferred to non-raft domains from raft domains by the MβCD treatment in 293T cells. However, the transfer of CXCR4 to non-raft domains by the MβCD treatment in NP2 and TE671 cells was not observed, because majority of CXCR4 molecules were originally localized to the non-raft domains in the cells.

To further assess the localization of CXCR4 in the plasma membrane, confocal laser scanning microscopy using the anti-CXCR4 antibody and CT-B was performed. In almost all 293T cells examined, CXCR4 was co-localized with CT-B, indicating that CXCR4 is largely localized to the raft domains in the MβCD-untreated 293T cells (Fig. 6B, the most upper panels). However, the fluorescent signals of the CXCR4 and CT-B were not matched in about 5% of MβCD-treated 293 T cells (Fig. 6B, the second panels). The data indicate that CXCR4 is partially transferred to non-raft domains by the MβCD treatment.

In contrast to the 293 T cells, the individual dot signals of CXCR4 were not completely matched to those of CT-B in the almost all TE671 cells (Fig. 6B, third panel, and arrows in the bottom panel). Interestingly, when two or more cells came in contact, CXCR4 molecules at cell–cell adhesion site appeared to be colocalized with CT-B (Fig. 6B bottom panel). The result may imply clustering of CXCR4 into raft domains at the

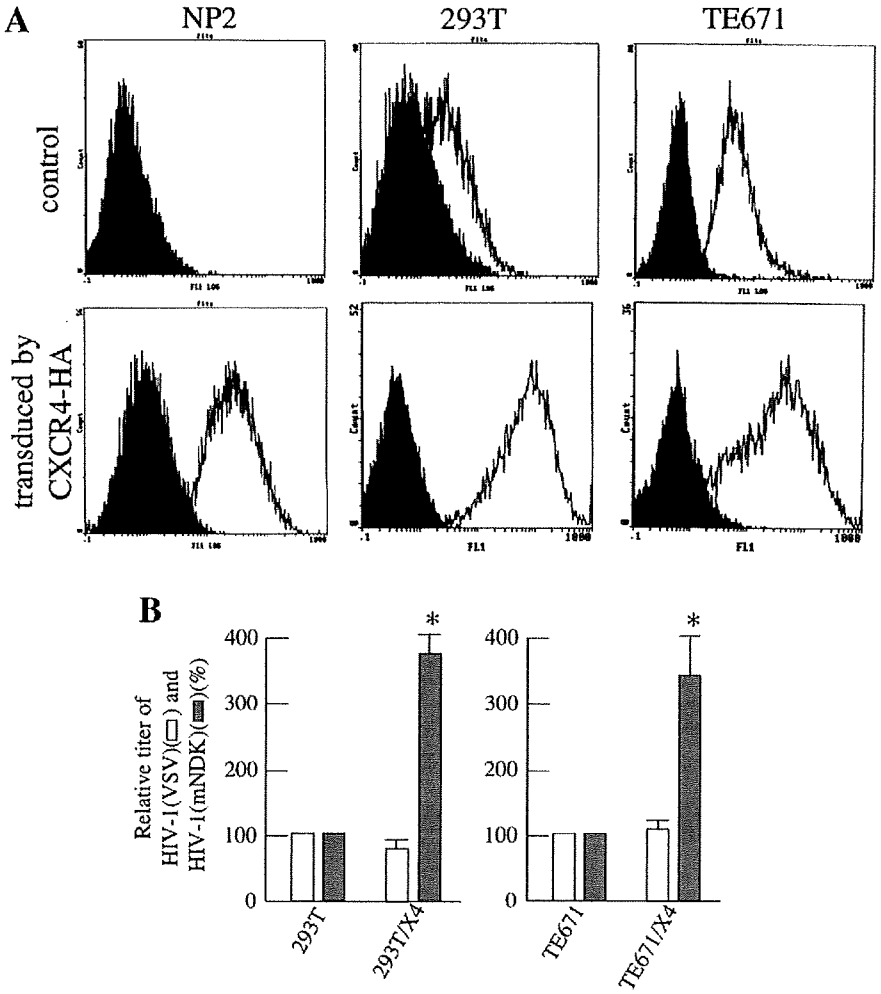

Fig. 2. Effect of CXCR4 overexpression on mNDK HIV-1 vector infection. (A) Cell-surface expression of CXCR4 in original NP2, 293 T, and TE671 cells and their CXCR4-overexpressing cells was analyzed by a flow cytometer using the anti-CXCR4 antibody (A80). Closed and open areas indicate the cells that were incubated in the absence and presence of the A80 antibody, respectively. (B) Relative transduction titers of the VSV-G (open bar) and mNDK (closed bar) vectors in the CXCR4-overexpressing cells to those in the original cells are indicated. This experiment was repeated three times and results are shown as means+SD. Asterisks indicate statistically significant differences compared to their controls.

cell–cell contact site, and is compatible with previous observations that contact between HIV-1 Env-expressing and receptor-expressing cells can induce translocation of CXCR4 from non-raft to raft regions (Manes et al., 2000; Nguyen et al., 2005), although the CXCR4 localization to raft domains at cell–cell contact site was independent of HIV-1 Env in our study. Raft localization of CXCR4 in NP2 cells could not be analyzed, because CT-B did not bind to NP2 cells. These results of cell-staining studies with the 293 T and TE671 cells were consistent with the results of cell fractionation studies of Fig. 6A.

MβCD inhibits soluble CD4-induced CD4-dependent infection

The MβCD treatment significantly inhibited the CD4-independent HIV-1 infection, but did not the CD4-dependent infection in the cells exogenously expressing CD4. To know whether the CD4-dependent infection does not require raft microdomains of the target cells, effect of MβCD on soluble CD4 (sCD4)-induced CD4-dependent infection was analyzed. In this experiment, CD4-dependent infection occurs independently of CD4 localization to raft domains. Interestingly, the MβCD treatment significantly inhibited the sCD4-dependent vector (NDK and HXB2) infection (Fig. 7), indicating that sCD4-induced CD4-dependent infection

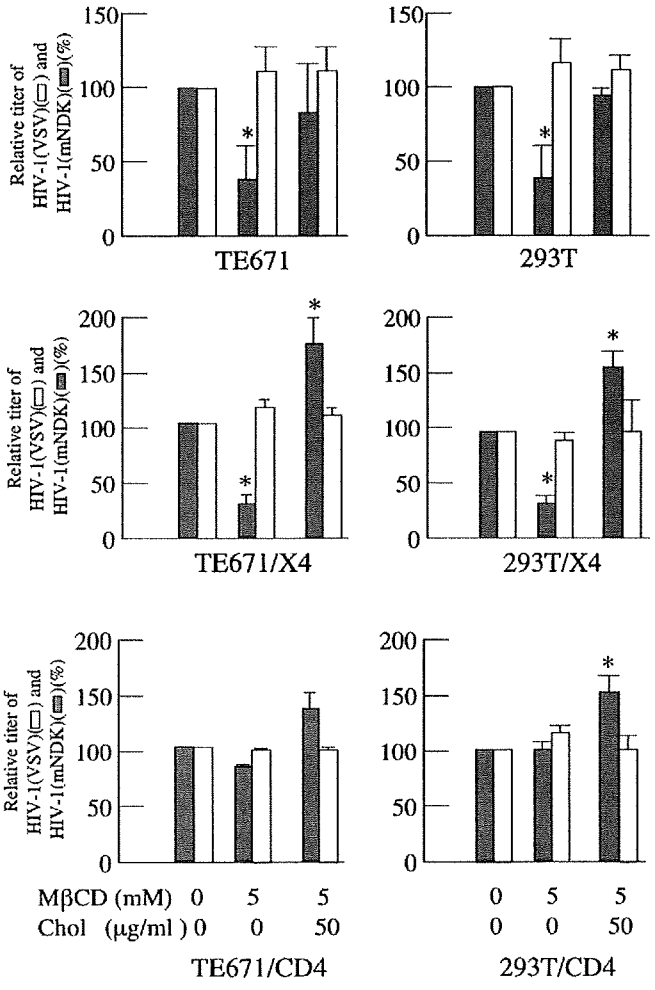

Fig. 3. Effects of MβCD on mNDK HIV-1 vector infection in CXCR4-overexpressing TE671 and 293T cells. Relative transduction titers of the VSV-G (open bar) and mNDK (closed bar) vectors in MβCD-treated, CXCR4-overexpressing TE671 and 293 T cells to those in untreated cells are indicated. Cells were treated with 0, 1, 5 mM MβCD for 30 min at 37 °C. Relative transduction titers to those in untreated cells are indicated. This experiment was repeated three times and results are shown as means+SD. Asterisks indicate statistically significant differences compared to their controls.

requires the raft membrane domains of the target cells. The result is compatible with the previous report that HIV-1 infection is inhibited by MβCD in cells expressing a CD4 mutant that is localized to non-raft domains (Popik and Alce, 2004).

Discussion

The raft domains are thought to participate in versatile biological events, such as signal transductions and cell–cell communications, as a scaffold for clustering particular membrane proteins. In this study, we examined potential roles of the raft in the X4-tropic HIV-1 infections. Previous puzzling observations (Del Real et al., 2002, Popik and Alce, 2004; Percherancier et al., 2003) prompted us to examine the possibility that raft localization of CXCR4 rather than CD4 is primarily required for X4-tropic HIV-1 infection. To avoid complications of CD4-dependent infection system, we used CD4-independent or sCD4-induced HIV-1 infection systems.

CD4-independent variants are thought to be prototypes of CD4-dependent variants, and to show fundamental entry pathway shared by both CD4-dependent and -independent viruses (Paolo, 2006; Kubo et al., 2007). Because the CD4-independent and sCD4-induced HIV-1 infections occur independently of CD4 raft localization, they are useful to study the function of CXCR4 raft localization in HIV-1 infection. The MβCD treatment significantly inhibited the CD4-independent (Fig. 1) and sCD4-induced CD4-dependent HIV-1 infections (Fig. 7). In addition, the CXCR4 over-expression did not affect the sensitivity of CD4-independent infection to the MβCD treatment (Fig. 3). These results indicate that raft localization of CXCR4 is required for these HIV-1 infections.

CXCR4 molecules were localized in the raft domains at cell–cell contact regions, but did not at exposed membrane regions (Fig. 6). The HIV-1 vector particles should bind to the CXCR4 molecules in the exposed cell surface regions, in which CXCR4 is localized to non-raft domains. How do the CXCR4 molecules present in non-raft domains function for the X4-tropic HIV-1 infection? It has been already reported that CXCR4 clusters to raft domains after HIV-1 binding to the cell surface receptors (Manes et al., 2000; Sorice et al., 2001; Del Real et al., 2002; Nguyen et al., 2005). Therefore, after the CD4-independent virus binds to CXCR4 in non-raft domains, the complexes could move and cluster in the raft domains and induce membrane fusion for the subsequent viral entry. Alternatively, binding of the CD4-independent HIV-1 to CXCR4 present in the raft domains, but not that in the non-raft domains, could induce productive infection. However, the latter possibility is unlikely, because CXCR4 in raft domains was detected in the unexposed cell–cell contact sites in TE671 cells, and NP2 and TE671 cells are as susceptible to the CD4-independent virus infection as 293T cells, in which CXCR4 is mainly localized to the raft domains. However, the CD4-independent infection in 293T cells was suppressed by MβCD as significantly as that in NP2 and TE671 cells. Because CXCR4 is originally localized to raft domains in 293T cells, the MβCD treatment could inhibit clustering the raft domains containing CXCR4 molecules in 293T cells. Taken together, clustering of the CXCR4 in raft domains should be important for the HIV-1 infection.

Why does the MβCD have no effect on the CD4-dependent infection in CD4-expressing cells? The lack of prominent inhibitory effect in our CD4-dependent infection system is compatible with previous study (Viard et al., 2002). The study showed that MβCD had no significant inhibitory effects on CD4-dependent infection when the cells expressed exogenously abundant amounts of CD4. One plausible explanation is that CD4 support the CXCR4 clustering in raft domains after the HIV-1 binding. The interaction of gp120 to CD4 could induce signals to recruit CXCR4 to cluster at the virus-binding site by regulating cytoskeleton dynamics (Iyengar et al., 1998; Viard et al., 2002; Kubo et al., 2008). It has been reported that the MβCD treatment slightly decreased cholesterol levels of the target cells (Lu

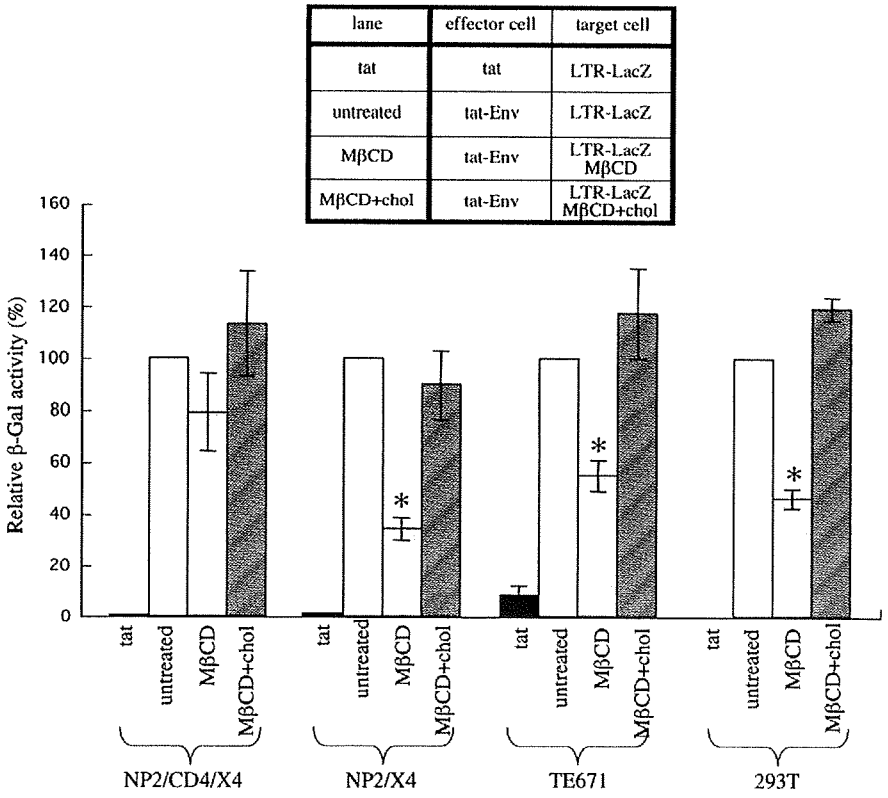

Fig. 4. Effect of MβCD on HIV-1 Env-mediated fusion. HEK293T effector cells were transfected with the tat or mNDK Env expression plasmid. The mNDK Env expression plasmid is designated as tat-Env, because it encodes the Tat protein as well as the Env protein. The target cells were transfected with the plasmids and treated by MβCD alone or both of MβCD and cholesterol as indicated in upper panel. These cells were mixed and LacZ activities of the cell lysates were measured as shown in Materials and methods. Relative values to LacZ activity of untreated cells were indicated. Asterisks indicate statistically significant differences compared to their controls.

et al., 2002), indicating that raft domains still exist in the MβCD-treated cells. Even the partial restriction of raft domains by MβCD should significantly inhibit the CD4-independent infection without the CD4 support, because certain numbers of the receptor molecules are required for the infection. Because the sCD4-induced infection was significantly inhibited by MβCD, the cytoplasmic domain-lacking sCD4 could not induce the signals. Further studies are needed to clarify this issue.

There are many evidence showing that the HIV-1 gp120–CD4-coreceptor complexes are clustered in the raft domains. However,

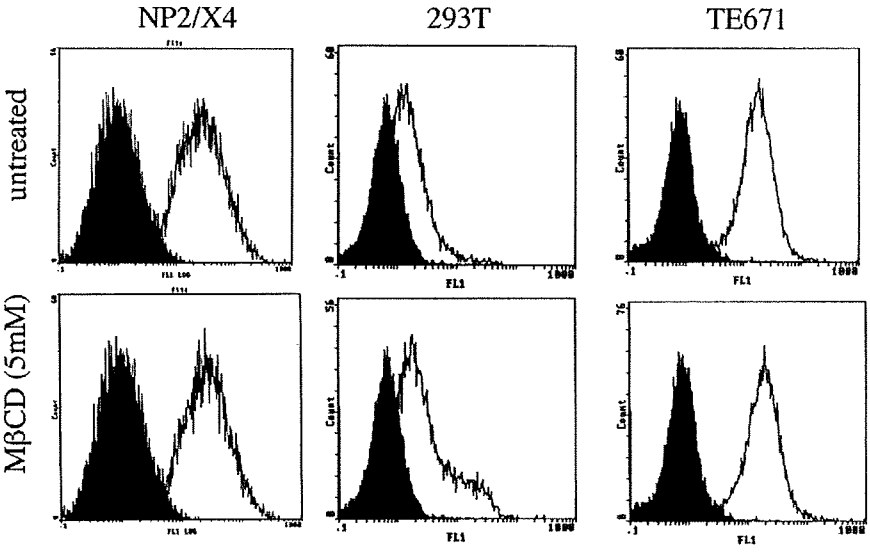

Fig. 5. Effect of MβCD on CXCR4 expression. Cell-surface expression of CXCR4 in NP2/X4, 293 T, and TE671 cells was analyzed by a flow cytometer. Upper panels indicate CXCR4 expression in untreated cells as control, and bottom panels indicate CXCR4 expression in MβCD-treated cells. Closed and open areas indicate cells that were incubated in absence and presence of the A80 antibody, respectively.

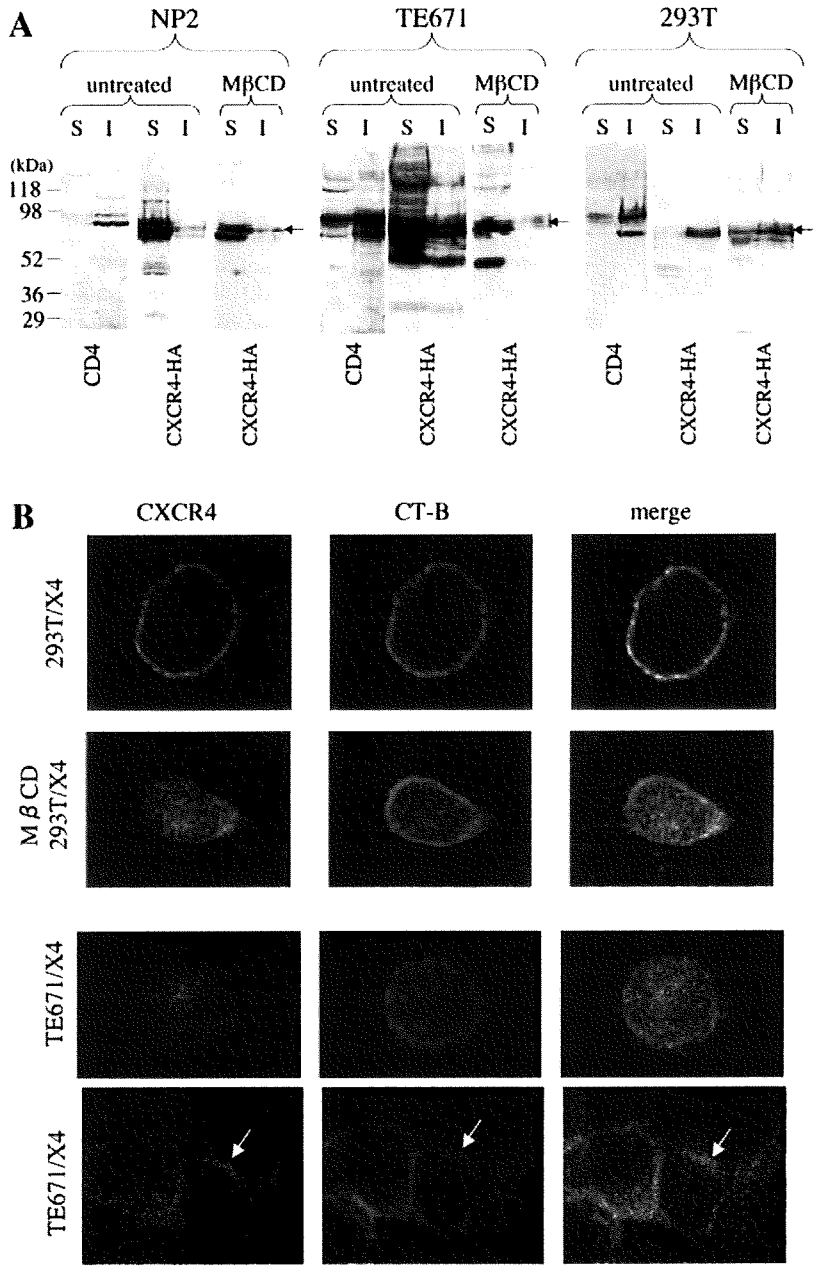

Fig. 6. Raft localization of CD4 and CXCR4 proteins in the different cells. (A) Cell lysates were prepared from MβCD-treated and untreated cells with 0.1% Triton X-100, and the soluble and insoluble fractions are defined as non-raft and raft domains, respectively as shown in Materials and methods. Cell lysates were electrophoresed on 7.5% polyacrylamide gels and Western blotting was performed using anti-CD4 and anti-HA antibodies. Molecular size standards are indicated on the left side of the panel. Arrows indicate CXCR4 molecules. (B) CXCR4 expressing cells were cultured on four-well culture slides for 24 h. MβCD-untreated (first panel) and treated (second panel) 293T/X4, and untreated TE671/X4 (third and forth panels) cells were incubated with the rat anti-CXCR4 antibody for 1 h at 4 °C, followed by AlexaFlour 555-conjugated CT-B (red) and FITC-conjugated anti-rat IgG (green) for 1 h at 4 °C. Representative results are shown. The colocalization of red and green gives yellow staining.

it is not clear what is the determinant for clustering the viral complexes in the raft domains. It has been reported that the CD4 mutants that do not localize to raft domains can support HIV-1 infection, and the HIV-1 infection through the CD4 mutants is sensitive to the MβCD treatment (Popik and Alce, 2004), indicating that CD4 is not the determinant. It was found in this study that the MβCD treatment significantly inhibits the CD4-independent X4-tropic HIV-1 infection, even when CXCR4 is over-expressed in the target cells, indicating that the raft localization of CXCR4 is absolutely required for the CD4-independent infection. In addition, the soluble CD4-induced HIV-1 infection was significantly inhibited by the MβCD treatment. These results provide that the raft localization of CXCR4, rather than CD4, is one of the key steps for the HIV-1 entry, and suggest that the interaction between the HIV-1 Env protein and the wild type CD4 supports the clustering of raft domains containing CXCR4.

Materials and methods

Env protein expression plasmids

The CD4-independent HIV-1 Env (mNDK strain) and its parental CD4-dependent HIV-1 Env (NDK strain) expression plasmids were